



Review

Generalized Odd-Even Mode Theory and Mode Synthesis Antenna Design Approach

Wen-Jun Lu

Jiangsu Key Laboratory of Wireless Communications, Nanjing University of Posts and Telecommunications, Nanjing 210003, China

Corresponding author: Wen-Jun Lu, Email: wjlu@njupt.edu.cn.

Received September 26, 2023; Accepted December 25, 2023; Published Online March 13, 2024.

Copyright © 2024 The Author(s). This is a gold open access article under a Creative Commons Attribution License (CC BY 4.0).

Abstract — In this article, studies on the multimode excitation problem of waveguides and antennas, the balance/unbalance mechanism and the balanced feeding techniques in dipole antenna systems are first briefly historically reviewed. In this context, generalized odd-even mode theory is advanced to quantitatively and approximately describe the mutual coupling effect between a feed line and an antenna. As is mathematically deduced and demonstrated, the modal parity mismatch between the feed line and the antenna should ultimately dominate the unbalance phenomenon in antenna systems. Thus, an elegant, closed-form formula is derived to approximately calculate the “unbalance degree” of a straight dipole off-center fed by a symmetric twin-wire line. Design approaches for the simplest, linear, 1-D multimode resonant antennas are introduced. Moreover, the “falling tone excitation” law gauged based on prototype dipoles is revealed and used to develop a mode synthesis design approach for microstrip patch antennas (MPAs) and 2-D sectorial electric dipole antennas. Design examples with distinctive radiation performance are presented and discussed. Finally, possible development trends of multimode resonant antennas are prospected.

Keywords — Generalized odd-even mode theory, Modal parity mismatch, Mode synthesis antenna design approach, Multimode resonant antenna.

Citation — Wen-Jun Lu, “Generalized odd-even mode theory and mode synthesis antenna design approach,” *Electromagnetic Science*, vol. 2, no. 1, article no. 0050441, 2024. doi: [10.23919/emsci.2023.0044](https://doi.org/10.23919/emsci.2023.0044).

I. Introduction

Excitation of waveguides and antennas is the most fundamental and classical problem in electromagnetic science and engineering. Studies on the concept of regularly shaped hollow waveguide tubes and their propagation modes can be dated back to 1897 [1]. Additionally, the basic behavior of multiple propagation modes within regular dielectric waveguide has been studied since 1910 [2]. These pioneering works laid the foundation for later waveguide and antenna theory under multimode resonance [3], [4]. Before the 1950s, because of the immaturity of electronic computers and lack of powerful numerical algorithms, the multimode excitation problems of certain regular waveguides and antennas were analytically treated by directly solving the governing partial differential equation (PDE) under specific boundary conditions or solving the PDEs/integral equations (IEs) with the aid of conformal mapping [5]. Alternatively, such a complicated electromagnetic field problem can be transformed into a circuit problem to be solved by using trans-

mission line theory [6], [7]. Classical transmission line theory is dominated by the telegrapher’s equations, in which only a single principal mode is assumed to be sufficiently excited to propagate [7].

That is, the feed line mode is supposed to perfectly match the antenna mode under the “single-mode transmission” condition; thus, the mode mismatch between them can be neglected. Transmission line theory under the “single-mode transmission, mode matching” premise may effectively simplify the analysis of electromagnetic problems, especially for antennas. When multiple propagation modes have to be considered in a problem, very complicated “generalized telegrapher’s equations” could be alternatively employed [8], [9]: In this case, a set of coupled transmission line equations could be derived to describe the mutual coupling effect between the principal mode and the propagating high-order modes.

Unfortunately, the premise of “single-mode transmission, mode matching” is only an ideal premise for simplify-

ing and facilitating theoretical analysis of electromagnetic problems. In practice, “multimode transmission, mode mismatching” should be the universally real condition. Typically, when a transmission line is connected to an antenna, the mode mismatch between them may excite an “unbalanced current” on the sheath of the transmission line as a result of interactions to partially “cancel” the mode mismatch effect. This current may yield undesired spurious cable radiation, pattern distortion, and various kinds of unexpected radiation performance degradations [10]. The coupling effect between a feed line and an antenna has been discussed in [10]. It can be analogously (but not equivalently) represented by a complicated circuit composed of multiple coupled resonant tanks. Thus, mathematical analytical treatment is unavailable [10] due to the complicated interconnected boundary conditions. Therefore, in an intuitive qualitative manner for practical applications, one of the main topics of [10] was “suppression of unbalanced currents”: The operational principle of quarter-wavelength sleeve chokes and detuning stubs was systematically illustrated.

Apart from some special cases in which unbalanced currents could be employed for beam manipulation [11], [12], these currents should be suppressed in most situations. The design, classification and assessment approaches for balancing devices (alternatively, balanced-to-unbalanced transformers, or “baluns”) have been extensively studied and remained an essentially important topic in microwave engineering, antenna theory, and electromagnetic compatibility [13]–[21]. In addition, a series of works have attempted to approximately calculate the unbalanced currents and the key parameters of balancing devices [22]–[28]. All of the design and analysis approaches are still based on the classical “single-mode transmission, mode matching” premise. Therefore, the unbalanced current is treated as a “parasitic component” in the antenna system and estimated based on experimental results [24] or approximate circuit models [25]–[28]. In general, elegant closed-form formulas for revealing the unbalance mechanism of an antenna system have seldom been reported.

To yield a new approach to study the unbalanced current in an antenna system and to design versatile multimode resonant antennas, generalized odd-even mode theory (GO-EMT) [29] based on the “multimode transmission, mode mismatching” premise must be advanced. Unlike the complicated generalized telegrapher’s equations based on classical transmission line and circuit theories [8], [9], the advanced GO-EMT can express the mutual coupling effect between a feed line and an antenna in a pure “field” fashion. Accordingly, a novel mode synthesis design approach for multimode resonant antennas can be systematically developed to yield distinctive, novel designs with different performance parameters. Design examples of 1-D and 2-D multimode resonant antennas will be introduced. Future challenging opportunities and possible development trends will be prospected and discussed. Some of the material in this article has been borrowed from the author’s book [29]

and invited conference presentation [30].

II. Generalized Odd-Even Mode Theory and 1-D Multimode Resonant Antennas

1. Generalized odd-even mode theory

In antenna theory, a feed line is generally modeled as a lumped source and emulated by the Dirac delta function $\delta(\vec{r}-\vec{r}')$ in the spectral domain, where \vec{r}' generally denotes the coordinate of the symmetric center of the antenna. When the feed line is to be connected to an antenna, the impulse function is expanded in terms of the eigenmode functions of the antenna in the spectral domain [31], [32].

Note that the Dirac delta function is an even-symmetric function. However, straight symmetric dipole antennas can exhibit both odd and even symmetries, corresponding to eigenmode sets of cosine and sine functions, respectively [33]. Therefore, speculating that the lumped source function of the feed line could be classified into “even” and “odd” types is reasonable: the even-symmetric Dirac delta function $\delta(\vec{r}-\vec{r}')$ and the odd-symmetric Dirac doublet function $\delta'(\vec{r}-\vec{r}')$.

As noted in [29], the surface current/field distributions of an antenna under multimode even- and odd-symmetric excitations can be represented by solving the Helmholtz’s equation and the associated homogeneous boundary conditions:

$$(\nabla^2 + k_{ne}^2)G_e(\vec{r}) = \delta(\vec{r}-\vec{r}'), \quad aG_e + b \frac{\partial G_e}{\partial r} \Big|_{\partial\Omega} = 0 \quad (1a)$$

$$(\nabla^2 + k_{no}^2)G_o(\vec{r}) = \delta'(\vec{r}-\vec{r}'), \quad aG_o + b \frac{\partial G_o}{\partial r} \Big|_{\partial\Omega} = 0 \quad (1b)$$

where Ω indicates the finite volume occupied by the antenna, $\partial\Omega$ denotes the bounded surface of Ω , and a and b are arbitrary constants. For brevity and without loss of generality, only the 1-D antenna case is considered herein, and the 2-D and 3-D cases can be elaborated in a similar way [29]. The resultant surface current/field distribution function is readily named the “interior Green’s function”. According to the spectral expansion in terms of eigenmode functions [29]–[32], the interior Green’s function can be respectively expanded and represented as the even- and odd-symmetric parts:

$$G_e(\vec{r}, \vec{r}') = \sum_n \frac{\psi_{ne}(\vec{r}')\psi_{ne}(\vec{r})}{(k_{ne}^2 - k^2)\|\psi_{ne}\|^2} \quad (2a)$$

$$G_o(\vec{r}, \vec{r}') = \sum_n \frac{-\psi'_{no}(\vec{r}')\psi_{no}(\vec{r})}{(k_{no}^2 - k^2)\|\psi_{no}\|^2} \quad (2b)$$

where $\{\psi_{ne}(\vec{r})\}$, $\{k_{ne}^2\}$, $\{\psi_{no}(\vec{r})\}$, and $\{k_{no}^2\}$ denote the even- and odd-symmetric eigenfunction and eigenvalue sets.

In this regard, the interior Green’s function expressed in an eigenspectral expansion fashion can be distinguished from the “Green’s function” in free space, open space or the half-open space widely used in traditional electromagnetic radiation and scattering problems [29]. This function should

indicate the surface current/field distributions of an antenna. Therefore, GO-EMT should be regarded as a creative expansion of classical, “interior”, guided-wave problems [1]–[4] by considering the parities of both the feed line and antenna.

According to (2), the feed line source functions are projected into the eigenspectral domain of the antenna. The excitation of each eigenmode can be determined by the projection amplitudes, i.e., the spectral coefficients. For a symmetric dipole fed at its symmetric center, the even-symmetric source dipole function can excite the eigenmodes with the same parity, and similarly for the odd-symmetric source function [29]. In particular, for an ideal, z -oriented, straight electric dipole fed at its center ($z = 0$) by a symmetric twin-wire line, only the cosine-dependent, even-symmetric modes can be sufficiently excited, with all sine-dependent, odd-symmetric modes completely suppressed [29], [34]: In this case, the twin-wire feed line (i.e., the source) can be emulated by the Dirac delta function, with projections on all the cosine-dependent modes at $z = 0$ of unity; thus, all even-symmetric modes can be sufficiently excited. Naturally, the feed line projections on all the odd-symmetric, sine-dependent modes at $z = 0$ should always be zero, so these modes would never be excited. This is exactly the “balanced situation” required in antenna engineering, and perfect mode matching between the feed line and antenna may guarantee this situation.

When the dipole is off-center fed at an arbitrary position along one arm, the situation is quite different. As shown in Figure 1(a), the feed position no longer coincides with the symmetric center \vec{r}' but has an off-center separation of ξ ; thus, the source function may project onto both even- and odd-symmetric eigenmode functions due to the breaking of the modal parity. That is, an even-symmetric source may partially excite the odd-symmetric eigenmodes with nonzero spectral coefficients, and vice versa. Mathematically, the interior Green’s functions under off-center feeding can be alternatively represented by

$$\begin{aligned} G_e(\vec{r}, \vec{r}' + \xi) &= G_{ee'}(\vec{r}, \vec{r}' + \xi) + G_{eo'}(\vec{r}, \vec{r}' + \xi) \\ &= \sum_n \frac{\psi_{ne}(\vec{r}' + \xi)\psi_{ne}(\vec{r})}{(k_{ne}^2 - k^2)\|\psi_{ne}\|^2} - \sum_n \frac{\psi'_{ne}(\vec{r}' + \xi)\psi_{ne}(\vec{r})}{(k_{ne}^2 - k^2)\|\psi_{ne}\|^2} \end{aligned} \quad (3a)$$

$$\begin{aligned} G_o(\vec{r}, \vec{r}' + \xi) &= G_{oe'}(\vec{r}, \vec{r}' + \xi) + G_{oo'}(\vec{r}, \vec{r}' + \xi) \\ &= \sum_n \frac{\psi_{no}(\vec{r}' + \xi)\psi_{no}(\vec{r})}{(k_{no}^2 - k^2)\|\psi_{no}\|^2} - \sum_n \frac{\psi'_{no}(\vec{r}' + \xi)\psi_{no}(\vec{r})}{(k_{no}^2 - k^2)\|\psi_{no}\|^2} \end{aligned} \quad (3b)$$

As indicated in (3a) and (3b), both the even- and odd-symmetric interior Green’s functions may include the cross-coupling terms $G_{eo'}$ and $G_{oe'}$, where the previous subscript denotes the eigenmode parity, and the later subscript with a prime denotes the source parity. In the center-fed case of $\xi = 0$, the cross-coupling terms $G_{eo'}$ and $G_{oe'}$ in (3a) and (3b) vanish; thus, $G_{ee'}$ and $G_{oo'}$ degenerate into G_e and G_o in (2a) and (2b), respectively.

An off-center feeding configuration would clearly

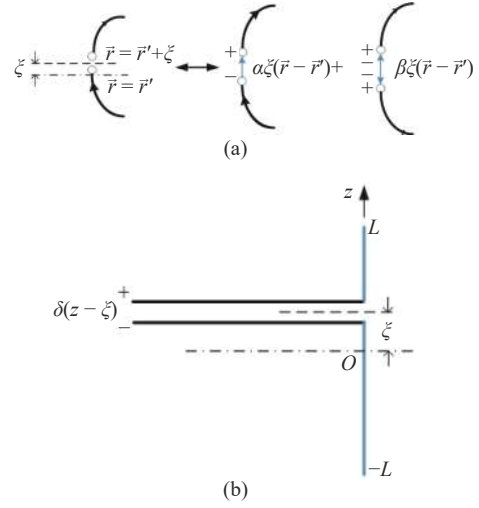


Figure 1 (a) General representation of an off-center-fed dipole; (b) Straight electric dipole antenna off-center fed by a twin-wire line.

break the symmetry of an antenna system; thus, nonzero, cross-coupling terms might be yielded in the interior Green’s function. Such cross-coupling terms are the mathematical expression of the “unbalanced component” in an antenna system [29]. Thus, the mutual coupling effect [10] can be quantitatively described by (3).

Using (2) and (3), the effect caused by the off-center feeding can be calculated using the coefficients of even-symmetric and odd-symmetric components; thus, the “unbalance degree” of an antenna system can be possibly defined and evaluated. Without loss of generality and for a better understanding, the simplest electric dipole antenna system in Figure 1(b) is considered herein: The ideal, z -oriented, straight electric dipole with a length of $2L$ is off-center fed at $z = \xi$ ($0 < \xi < L$) by a symmetric twin-wire line. In this case, the feed line is emulated by a Dirac delta function, and it may partially excite the odd-symmetric, sine-dependent eigenmodes. Thus, the interior Green’s function of the dipole can be expressed as

$$\begin{aligned} G(z, \xi) &= G_{ee'}(z, \xi) + G_{oe'}(z, \xi) \\ &= \sum_{n=1}^{\text{odd}} \frac{\cos \frac{n\pi}{2L}\xi \cos \frac{n\pi}{2L}z}{\left(\frac{n\pi}{2L}\right)^2 - k^2} + \sum_{n=2}^{\text{even}} \frac{\sin \frac{n\pi}{2L}\xi \sin \frac{n\pi}{2L}z}{\left(\frac{n\pi}{2L}\right)^2 - k^2} \end{aligned} \quad (4)$$

The even-symmetric and odd-symmetric parts of (4) can be truncated to maintain the first term for approximation. In this regard, the truncated interior Green’s function can be approximately written as

$$\begin{aligned} G(z, \xi) &\approx \frac{\cos\left(\frac{\pi}{2L}\xi\right)\cos\frac{\pi}{2L}z}{\left[\left(\frac{\pi}{2L}\right)^2 - k^2\right]} + \frac{\sin\frac{\pi}{L}\xi\sin\frac{\pi}{L}z}{\left[\left(\frac{\pi}{L}\right)^2 - k^2\right]} \\ &= c_{ee'}\cos\frac{\pi}{2L}z + c_{oe'}\sin\frac{\pi}{L}z \end{aligned} \quad (5)$$

Using (5), the ratio of the Fourier coefficients of the approximate, single-term truncated even-symmetric and

odd-symmetric series can be defined as the “unbalance degree” of the dipole antenna system shown in Figure 1(b), which can be expressed as

$$u(k, \xi) = \frac{c_{oe'}}{c_{ee'}} = 2 \sin \frac{\pi}{2L} \xi \frac{\left(\frac{\pi}{2L}\right)^2 - k^2}{\left(\frac{\pi}{L}\right)^2 - k^2} \quad (6)$$

When the antenna is center-fed ($\xi = 0$), the function $u(k, \xi)$ in (6) yields zero, which means that the antenna system should be “balanced”. When the separation ξ is approaching one end of the dipole ($\xi \rightarrow L$), the sine function in (6) may approach unity, which implies “unbalance”. The unbalance degree is also frequency-dependent, as illustrated in (6). In this manner, the mutual coupling effect between the feed line and antenna can be approximately described by the closed-form expression of (6). Although the primary expression of (6) is rough and approximate, it provides a quantitative tool to intuitively reflect the mathematical nature of and clearly reveal physical insights into the “unbalance phenomenon” in the simplest antenna system. The unbalance degree of other simple antenna systems can also be deduced in a similar analytical way. The developed analytical approach and approximate expression should be beneficial for a better mathematical and physical understanding of complex antenna designs [31].

As discussed in [10], the unbalanced current should flow along the outer surface of the feed line to cancel the modal parity mismatch effect between the feed line and antenna. Therefore, the unbalanced current should run orthogonal to the antenna current. Such “orthogonality” may be mathematically explained by the orthogonality of the cosine and sine series in (4) and (5). The unbalanced current owing to the partial excitation of odd-symmetric eigenmodes (especially, and most importantly, the 2nd-order, full-wavelength mode) may co-dominate the antenna system radiation behavior with the normal balance antenna currents, thus leading to a high cross-polarization level and beam squint. As evidence, significant beam distortion and a high cross-polarization level in principal-cut planes can be observed when an off-center-fed configuration is employed to design a wideband antenna [35]. The unpredicted radiation performance degradations in an unbalanced, complex antenna system [11], [14] can be generally termed “the hot-cable effect” [36].

The orthogonality of the feed line and antenna currents illustrated by (4) and (5) is also compatible with the generalized telegrapher’s equations in [8], [9]: The antenna field/current corresponds to the “transverse” waveguide field/current (expanding the cosine series), and the feed line field/current corresponds to the “longitudinal” field/current flowing along the center conductor (expanding the sine series) [9]. GO-EMT relies on the intrinsic parities of an antenna and its feed line, i.e., the parities of the eigenmode function family and the excitation, respectively. This theory can be deduced according to the “multimode transmission, mode mismatching” premise. This approach yields an

elegant but approximate closed-form formula of (6) to quantitatively estimate the unbalance performance of an off-center twin-wire line-fed electric dipole antenna system. The idea of considering the parities of the “antenna” and “feed” may be extended to estimate the “unbalance degree” of other simple antenna systems, e.g., the coaxial-cable-fed electric dipole and the probe-fed magnetic dipole. Thus, the advanced GO-EMT should be logically self-consistent and compatible with those classical antenna theories pioneered by Schelkunoff [8], [9] and King [10]. The simplified, semi-analytical GO-EMT model is still valid for other arbitrarily complicated antenna systems with symmetry in at least one dimension, e.g., an airplane [37], since it reflects the mathematical nature based on the simplest expression of (6). Several qualitative remarks and design guidelines have also been presented in [29] according to GO-EMT, which can be directly employed to instruct the feed schemes of multimode resonant antennas and to develop a mode synthesis antenna design approach. These remarks and design guidelines inspired the research and development of 1-D multimode resonant antennas with the simplest, straight-line configuration. Then, they motivated the quantitative semi-analytical mode synthesis antenna design approach for 2-D multimode resonant antennas presented in the next section.

2. 1-D multimode resonant antennas

Within the theoretical framework of GO-EMT, the multimode resonance concept has been employed to design elementary antennas with the simplest configuration. Multimode design approaches for the simplest, 1-D linear electric/magnetic dipoles have been developed since 2015 [38]–[68]. In the development of linear antennas under multimode resonance, it was found that the length the multimode resonant dipole should be approximately set to 1 wavelength [69] so that the high-order modes can be simultaneously excited with the fundamental mode.

A slotline antenna was the first type of dual-mode resonant antenna implemented [38]–[42]. As defined, “slotline” indicates that the length of a rectangular slot radiator must be much larger than its width to guarantee a slim, linear, 1-D profile. Conceptually, for a center-fed slotline antenna, the first three odd-order (1st, 3rd and 5th) modes can be simultaneously excited and tuned to implement wideband or multiband operations. When the slotline antenna is off-center fed, even-order modes can be partially excited to yield gain frequency notch characteristics while maintaining a continuous wide impedance bandwidth [40].

As illustrated in Figure 2(a), the high-order modes can be perturbed downward from their fundamental counterpart by incorporating slotline stubs near the respective surface E-field distribution nodes [38], [39], [41]. Alternatively, the fundamental mode can be tuned upward from its high-order counterpart by loading a pair of short-circuited strips near the surface E-field distribution nodes of the third-order resonant mode [40]. Selective prototypes are given in Figure 2(b). Table 1 compares the resultant impedance bandwidths of the multimode resonant slotlines with the

simplest, symmetrically fed configurations. As can be seen, the impedance bandwidth can be remarkably enhanced to over 30% by sufficiently exciting the intrinsic resonant modes within a single slotline radiator, without introducing external accessories or impedance matching networks. If more degrees of freedom in design can be properly incorporated, then a wider bandwidth and more novel functionalities can be implemented.

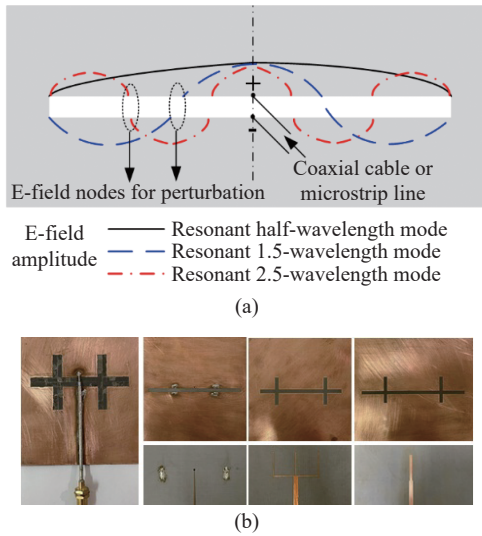


Figure 2 Multimode resonant slotline antennas. (a) Conceptual illustration of multimode resonance; and (b) Fabricated prototypes.

Table 1 Impedance bandwidth comparisons of the simplest slotline antennas under symmetric feeding

Ref.	Number of resonant modes	Impedance bandwidth
[38]	2	31.5%
[39]	2	32.7%
[40]	2	37.6%
[41]	3	33.2%

Since the multimode resonance concept for slotline antennas was proposed in 2015, this type of antenna has been further developed to yield versatile wideband and multi-band antenna/circuit designs [43]–[53]. Since 2016, the multimode resonance concept has been reported to be employed in the design of microwave switches [43], wideband or multiband mobile terminal antennas [44]–[48], radio frequency identification (RFID) antennas [49], etc. Other multimode design approaches [50]–[53] have also been developed, such as the characteristic mode approach based on the numerical method of moments (MoM) [50] and the mode compression approach [51]–[53] with the aid of dielectric loadings.

According to the complementary principle of electromagnetics, multimode resonant electric dipole antennas can be designed and implemented. Electric dipoles [54] and monopoles [55] under multimode resonance have been investigated. As illustrated in Figure 3(a), the high-order dipole modes can be perturbed downward from their fundamental counterpart by incorporating stubs near their sur-

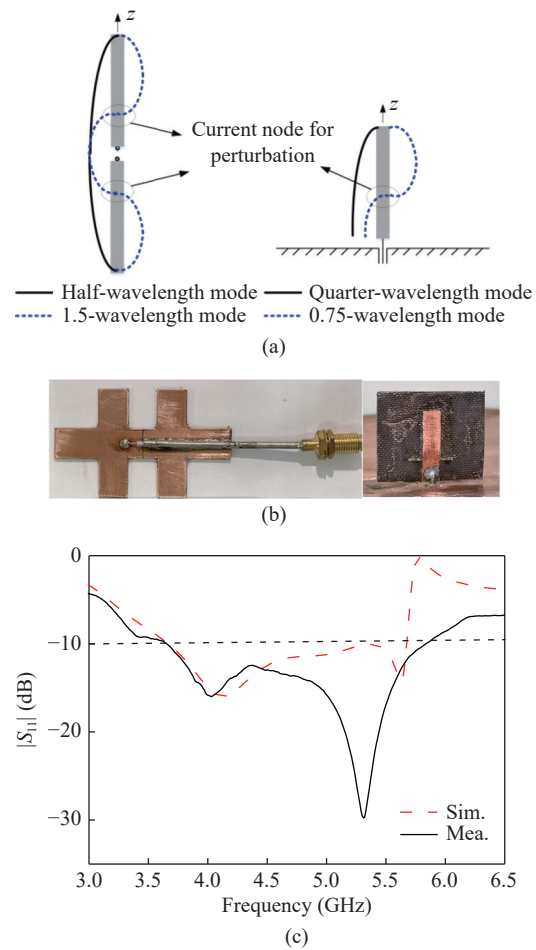


Figure 3 Multimode resonant electric dipole and monopole antennas. (a) Conceptual illustration of multimode resonance; (b) Fabricated prototypes; and (c) Measured and simulated $|S_{11}|$ of the printed monopole antenna.

face electric current distribution nodes, and the fundamental mode can be tuned upward by etching interdigital capacitors at the same positions [52]. The orthogonally loaded stubs may make the dipole more bulky and not suitable for compact designs [54].

For a more compact size, the loaded stubs can be shortened by using lumped inductors [55]: Unlike the classical compact monopole design approach in which the lumped element should be loaded along the main monopole [56], the lumped elements for compact size design can be alternatively loaded on the tuning stubs. In this manner, the principal monopole is not truncated by the loaded lumped element, and the stub length can be reduced by 65% to yield a smaller size [55]. Figure 3(b) presents some of the fabricated dipole and monopole antennas. As reported in [54], [55], the dual-mode resonant electric dipole or monopole under the simplest basic configuration can exhibit an impedance bandwidth of over 40% [54], [55]. If a dielectric substrate is loaded to yield a single-layer printed version, then an impedance bandwidth of approximately 60% can be realized [29], as illustrated in Figure 3(d).

Numerical investigations and designs of multimode resonant electric dipoles have been developed since the

“single radiator, multimode resonance” concept was advanced in 2017 [57]–[64]. In addition to the extensive MoM investigations [57], the multimode electric dipole concept has been employed to design ultrawideband antennas [58], [59], wideband antennas for passive coherent location (PCL) [60] and borehole radar [61] applications, multiband antennas with filtering functionalities [62], [63], and compact broadband mobile base station antenna arrays [64]. Therefore, the design approach for multimode resonant electric dipole antennas has been widely used in various kinds of wireless applications.

Inherently, multimode resonant 1-D slotline and electric dipole antennas are linearly polarized (LP) because of their axial symmetry. A cross-dipole configuration can be employed to generate circularly polarized (CP) radiation. For CP operation, a center-symmetric, loop configuration is a good candidate since a pair of odd- and even-symmetric degenerate modes can be excited and utilized [29]. Therefore, loop antennas [65]–[69] under a pair of even-mode resonances have been developed to realize CP antennas. In this case, a pair of orthogonal even modes can be simultaneously excited to yield a pseudo-travelling-wave current distribution [29], which is quite similar to that of the Kraus helix [70].

In this manner, a circular or square loop antenna under a pair of even-mode resonances may generate bidirectional CP radiation, which corresponds to the Poincaré sphere for partially polarized field representations [71]: As illustrated in Figure 4(a), the antenna radiates pure right-handed CP (RHCP) and right-handed elliptically polarized (RHEP) waves at the north pole and in the northern hemisphere, respectively, while it radiates pure left-handed CP (LHCP) and left-handed elliptically polarized (LHEP) waves at the south pole and in the southern hemisphere. In the equatorial plane, the antenna radiates LP waves [29]. Interchangeably, bidirectional CP radiation corresponding to an inverse Poincaré sphere can also be implemented by modifying the phase quadrature leading/lagging condition of the even modes. Thus, the simplest, bidirectional CP loop antennas under a pair of even-mode resonances can be reasonably named a “Poincaré sphere source antenna” [29]. Figure 4(b) illustrates the current distributions of each even mode, and Figure 4(c) plots the bidirectional balanced-fed [66], bidirectional unbalanced-fed [67], and unidirectional multiloop [68] prototypes.

Based on the operation principle of Poincaré sphere source antennas, more novel dual CP antennas have been developed in recent years. By using the combination of an even-mode resonant loop and an inverted-L monopole, dual-band, dual circular polarization characteristics can be implemented [72]. The hybrid loop-slot mode [29] can be utilized to implement a dual CP antenna system with high port isolation for full duplex communications, with the aid of a compact interdigital band stop filter [73]. The loop under even-mode resonance can be periodically loaded onto a microstrip patch antenna (MPA) to yield dual CP, high-gain, unidirectional antennas [74]. Wideband [75], dual-

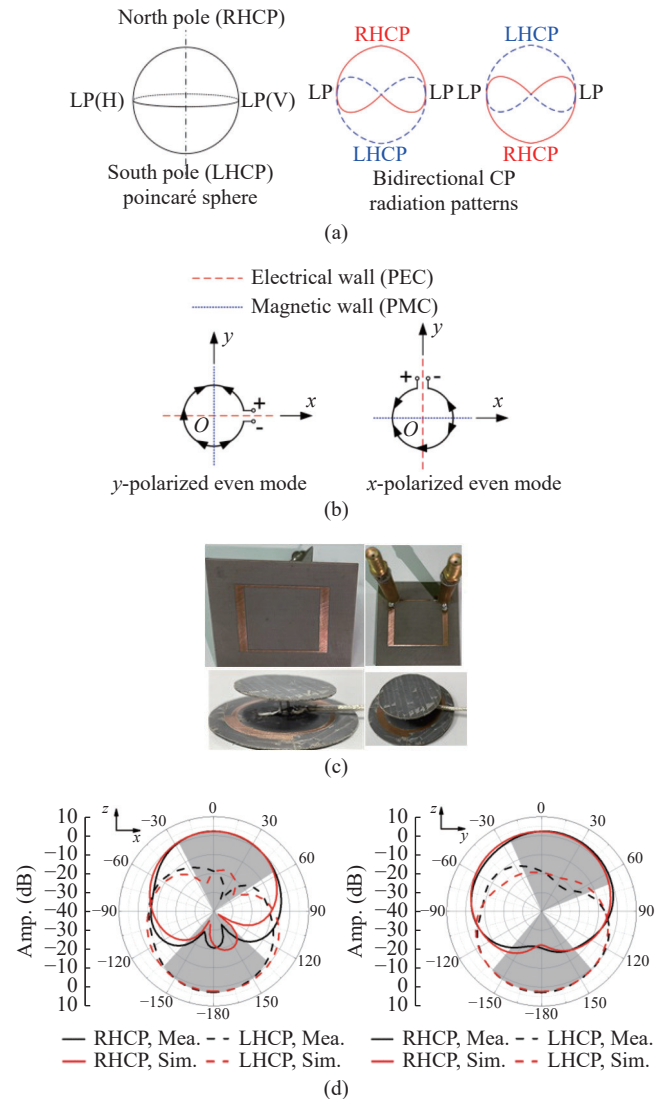


Figure 4 Poincaré sphere source antennas. (a) Illustration of the Poincaré sphere for the partially polarized field representation; (b) Conceptual designs; (c) Fabricated prototypes; and (d) Bidirectional CP radiation characteristics indicated by shadows.

band [76], [77] and miniaturized [78] Poincaré sphere source antennas have been developed. Compared to other types of CP antennas, the Poincaré sphere source antennas in the basic form can always exhibit a front-to-back ratio (FBR) as high as 25 to 40 dB [66]–[69], [74]–[78] even under unbalanced feeding, as illustrated in Figure 4(d).

The practical implementation and development of the simplest, linear, 1-D multimode resonant antennas have successfully validated the correctness and effectiveness of GO-EMT. For the linear 1-D antennas with the simplest, basic configurations, there is only one degree of freedom in design for manipulation, i.e., the length (slotline and electric dipole or monopole) or the circumference (loop). To invent more innovative multimode resonant antennas, planar 2-D configurations with more degrees of freedom in design should be employed. This yields a mode synthesis antenna design approach for the simplest 2-D multimode resonant antennas.

III. Mode Synthesis Antenna Design Approach and 2-D Multimode Resonant Antennas

1. Mode synthesis antenna design approach

The concept of “mode synthesis” is inspired by GO-EMT and boosted by the studies on 1-D and 2-D quasi-isotropic antennas. It has been analytically revealed that a U-shaped, quarter-wavelength dipole may exhibit null-free, quasi-isotropic radiation characteristics [79]. In practice, such a U-shaped dipole is hard to sufficiently excite because most of the electric currents flowing on each arm may cancel each other out, thus yielding an extremely low radiation efficiency, so this dipole is only meaningful as an initial prototype for theoretical analysis. To easily excite a U-shaped dipole, the vertical portion with the feed port can be aligned along the z -axis, with both horizontal arms rotated to a certain angle relative to the z -axis. Thus the 1-D, U-shaped dipole evolves into a 2-D circular sector magnetic dipole with flare angle α and both radii R short-circuited: This yields a 2-D resonant magnetic current cavity such that magnetic currents can be alternatively excited to generate quasi-isotropic radiation [80], rather than boost the mutually canceling currents on each arms [79]. The design process of quasi-isotropic, circular sector magnetic dipole antennas bridges 1-D linear antennas (U-shaped dipole) with 2-D planar antennas. It also reveals the basic excitation laws of the circular sector magnetic current cavity with two degrees of freedom in design, i.e., the flare angle α and the radius R , under the constraint of the circumferential length L [80], which yields the concept of “mode synthesis”.

Motivated by the evolution process in [80], MPAs under multimode resonances can be designed by mapping a prototype magnetic dipole to a circular sector microstrip radiator. In this manner, the 1-D, symmetric prototype magnetic dipole fit to the circumference may naturally yield 2-D, circular sector MPAs with different flare angles and radii, as illustrated in Figure 5(a). The modal parity of the MPA is determined by the boundary conditions of the prototype magnetic dipole. The resonant frequency of the first usable mode can be estimated either by the circumference length L or by the eigenvalue $\chi_{\nu,1} (\nu = n\pi/\alpha, n = 1, 2, \dots)$ of the circular sector patch [81], [82]. Thus, the prototype magnetic dipole can be employed to gauge the order of the excited mode and estimate the radius of the patch. When the difference between radii calculated by (7a) and (7b) is less than 0.1λ (λ denotes the center wavelength), the corresponding resonant mode can be readily determined to be excited [81], [82].

$$R = \frac{L}{\alpha} = \frac{n\lambda}{2\alpha}, \quad n = 1, 2, \dots \quad (7a)$$

$$R = \frac{\chi_{\nu,1}}{2\pi}\lambda, \quad \nu = \frac{n\pi}{\alpha}, \quad n = 1, 2, \dots \quad (7b)$$

Mathematically, the “mode gauge relation” illustrated by (7a) and (7b) can be explained by the analytical princi-

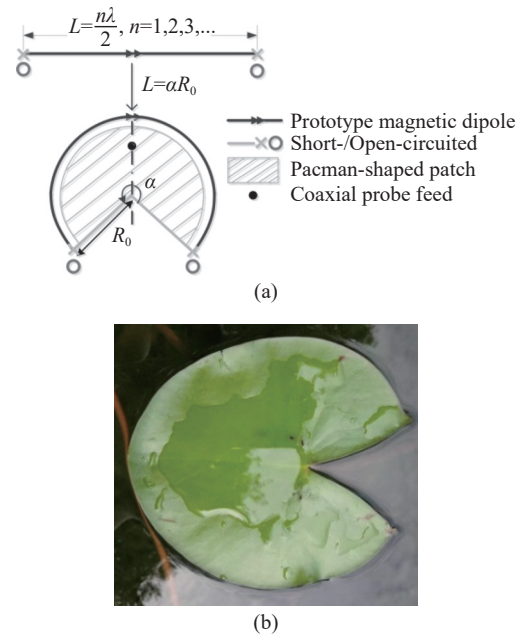


Figure 5 Mode synthesis antenna design approach. (a) Evolution from a 1-D prototype dipole to 2-D circular sector MPAs under the mode gauge relation; and (b) Natural Pacman resonator: a water lily (*Nymphaea L.*) pad (photographed in Xuanwu Lake, Nanjing, China).

ple of estimating the eigenvalues of an arbitrary closed, convex membrane or planar cavity according to the length of its caustic [83]: The circumference serves as the caustic of the circular sector radiator under whispering gallery mode resonance (i.e., $TM_{\nu,1}$ modes, with the latter radial index fixed to unity) such that the circumference L can be set to integer multiples of the one-half wavelength and employed to gauge the order of the usable resonant mode.

In the classical applied mathematical literature [84], [85], the yielded circular sector shape is usually called a “Pacman”. For a Pacman-shaped MPA, its eigenmodes can be analytically expressed by the Fourier-Bessel series [82]. The Pacman-shaped resonator can also be evolved into resonators of other shapes owing to its general eigenfunction family dominated by the Fourier-Bessel series [85], [86]. Pacman-shaped resonators can be naturally found in many wild plants, as intuitively illustrated by the water lily (*Nymphaea L.*) pad in Figure 5(b); the leaf floating on or immersed in water can be modeled as a Pacman membrane with a free circumference (i.e., the Neumann boundary condition), and its forced vibration can be mathematically depicted by the eigenmode family in the Fourier-Bessel form [81]–[86]. To some extent, the Pacman-shaped MPAs can be speculated to be one of the simplest, naturally shaped MPAs with two degrees of freedom in design (i.e., flare angle α and radius R). They can be analytically designed by using the mode synthesis design approach [29], [30], [34], [81], [82].

2. 2-D multimode resonant antennas

The mode synthesis antenna design approach has been employed to design and implement Pacman-shaped MPAs and

sectorial electric dipole antennas. As gauged based on the mode synthesis tables and charts [29], [30], [81], [82], the “falling tone excitation” law can be observed: A 1.0-wavelength prototype dipole may be gauged to excite the fundamental mode of the radiator, a 1.5-wavelength prototype dipole may be gauged to excite the 2nd-order mode, a 2.0-wavelength prototype dipole may be gauged to excite the 3rd-order mode, and so on. For LP Pacman-shaped MPAs, high-order modes having similar parity to the first gauge mode will be accordingly excited, perturbed and utilized. Design examples are introduced in the following.

When a 1.5-wavelength magnetic dipole with both ends open-circuited is employed to gauge the usable mode of a Pacman-shaped MPA, the high-gain MPA design shown in Figure 6(a) is yielded [81]. Unlike conventional rectangular/circular MPAs resonating at the fundamental mode, the high-gain Pacman-shaped MPA operates at its 2nd-order and 4th-order modes, with the fundamental mode automatically and fully suppressed. The antenna under pure high-order mode resonances is implemented by the intrinsic symmetry properties of the radiator and the boundary conditions of the prototype dipole: In this resultant Pacman-shaped MPA, all even-order modes are even-symmetric, and they can be directly excited by a coaxial probe placed at its angular bisector, with all odd-order, odd-symmetric modes automatically suppressed. Alternatively, a horizontal coupled aperture parallel to the angular bisector etched on the ground plane may be employed to excite the odd-order modes instead. Since pure high-order modes are excited, the antenna operates with a larger effective aperture than its fundamental-mode-resonant counterparts, thus leading to a high gain of up to 10.7 dB [81].

A full-wavelength magnetic dipole with both ends short-circuited is employed to yield a MPA with a widened beamwidth under dual, odd-order mode resonances [82], [87]–[89], with fabricated prototypes shown in Figure 6(b). In this case, the fundamental mode and its 3rd-order counterpart can be simultaneously tuned and utilized to yield a broadened E-plane beamwidth of up to 120° [82], [87], which is much wider than the typical value of 60° for conventional MPAs on an air substrate. Alternatively, the radially symmetric TM_{01} and TM_{02} mode-resonant, circumferentially short-circuited circular sector patch antenna may also exhibit a widened beamwidth: The prototype magnetic dipole should be gauged in the radial direction (i.e., the caustic [83] orthogonal to the circumference), and the excited TM_{01} and TM_{02} modes should be analogous to the “bouncing ball” modes in [83]. In this case, the E-plane beamwidth can be widened to 128° [88], [89].

An asymmetric, circumferentially set prototype dipole may yield Pacman-shaped MPAs with one radius open-circuited and the other short-circuited. As a result, the order of the resonant modes should be reduced by one-half from $n\pi/\alpha$ ($n = 1, 2, 3, \dots$) to $n\pi/2\alpha$ ($n = 1, 3, 5, \dots$), and the length of the prototype dipole should be set as an odd-number multiple of the one-quarter wavelength [90]. Thus, Pacman-

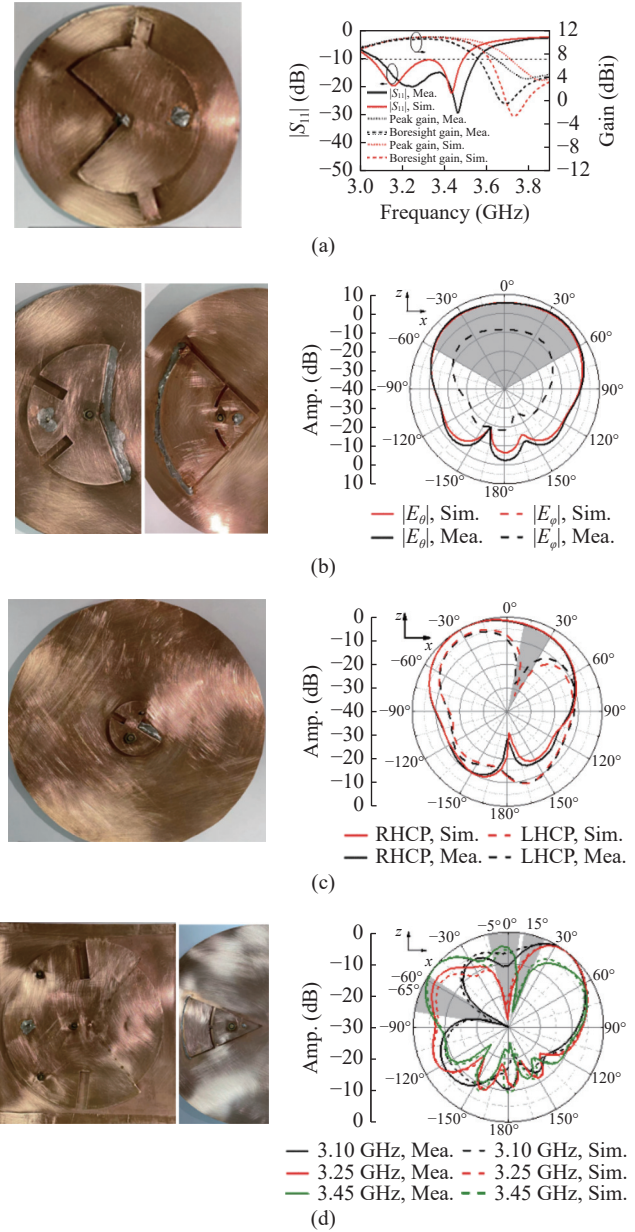


Figure 6 Pacman-shaped MPAs implemented through the mode synthesis design approach. (a) High-gain antenna with a gain up to 10.7 dBi; (b) Wide-beamwidth antennas with a half-power beamwidth of 120° ; (c) Tilted-beam CP antenna with a miniaturized patch and a tilted CP angle of $\theta = 25^\circ$; and (d) Null frequency scanning antennas with a scanning range of $\theta = -65^\circ - (+15^\circ)$.

shaped MPAs having a tilted CP beam with a reduced patch size are yielded. By incorporating a longer, 1.25-wavelength prototype dipole, a higher gain and a larger CP tilt angle can be attained. Figure 6(c) plots some fabricated prototypes.

The preceding Pacman-shaped MPAs [81], [82], [87]–[90] are synthesized and designed based on prototype magnetic dipoles no longer than 1.5 times the wavelength. When the length is fitted along the circumference and increased to 2.0 times the wavelength, the resultant MPAs may resonate at their 3rd-order mode. In this case, the 1st-,

3rd- and 5th-order modes can be simultaneously tuned and manipulated to yield frequency-dispersive, null frequency scanning antennas (NFAs) [91], [92]. As the frequency is varied, the radiation null can be continuously scanned from a positive elevation angle to negative elevation angle without a scanning blind zone. Thus, the NSAs in [91], [92] should possess a negative frequency scanning slope and a flare-angle-dependent frequency scanning sensitivity. By gauging with an asymmetric, 1.75-wavelength prototype dipole in the radial direction and exciting multiple radially symmetric TM_{0x} ($x = 1, 2, 3$) modes, NSAs with a positive frequency scanning slope can be designed and implemented instead. Unlike the circumferentially resonant cases in [91], [92], the radiation null may exhibit a “double-slope” frequency scanning characteristic: It exhibits high/low sensitivity in the low-/high-frequency band and a negative/positive elevation angular range, respectively [93]. Some of the fabricated NSAs are illustrated in Figure 6(d).

Without loss of generality, selected Pacman-shaped MPAs are compared with their respective counterparts [94]–[103]. As tabulated in Tables 2, 3 and 4, the wideband Pacman-shaped MPAs can exhibit a wideband performance superior or comparable to that of their counterparts with the fewest design parameters. More comprehensive comparisons have been given in [81], [89], [93].

The mode synthesis design approach for multimode resonant MPAs can be extended to the design of 2-D electric current sheets, i.e., sectorial electric dipoles [29], in a complementary manner. Correspondingly, the Pacman-shaped patch may be symmetrically evolved into the two arms of the sectorial dipole with ground plane removal, and the operational mode may change from TM to TE modes

[104]. Thus, TE circumferentially resonant sectorial dipoles can be designed using the mode synthesis charts/tables [81], [82] in the same way. Similar to the 1-D electric and magnetic dipole antennas, the sectorial electric dipole under dual TE mode resonances can exhibit a wider operational bandwidth than its magnetic counterpart. Figure 7 illustrates some fabricated prototypes of sectorial dipoles under multiple-mode resonance. As validated in the sub-6 GHz mobile communication band, a dual-mode resonant sectorial electric dipole can exhibit an available bandwidth of over 50% in the simplest, basic form [104].

Table 2 Comparisons of high-gain antennas (N.A. = not available)

Ref.	Number of design parameters	Impedance bandwidth	Gain (dBi)	Size
[81]	8	14.5%	10.7	$1.03\lambda_g^2 \times 0.05\lambda_g$
[94]	9	1.8%	11.7	$1.18\lambda_g^2 \times 0.02\lambda_g$
[95]	6	2.6%	11.0	$0.38\lambda_g^2 \times 0.03\lambda_g$
[96]	27	12.0%	8.6	$4.45\lambda_g^2 \times 0.1\lambda_g$
[97]	N.A.	29.6%	7.6	$1.82\lambda_g^2 \times 0.12\lambda_g$

Table 3 Comparisons of wide-beamwidth antennas

Ref.	Number of design parameters	Impedance bandwidth	Beamwidth	Size
[82]	8	25.0%	120°	$0.15\lambda_g^2 \times 0.043\lambda_g$
[89]	8	17.4%	128°	$0.31\lambda_g^2 \times 0.03\lambda_g$
[98]	16	13.4%	126°	$3.51\lambda_g^2 \times 0.7\lambda_g$
[99]	11	3.0%	107°	$0.04\lambda_g^2 \times 0.07\lambda_g$
[100]	13	34.8%	101°	$0.81\lambda_g^2 \times 0.4\lambda_g$

Table 4 Comparisons of null frequency scanning antennas (S.A. = specified angle)

Ref.	Number of design parameters	Impedance bandwidth	External feed accessories	Scanning range	Size
[91]	10	24.0%	N	$\theta = 35^\circ$ to -60°	$0.57\lambda_g^2 \times 0.04\lambda_g$
[93]	8	34.3%	N	$\theta = -90^\circ$ to 45°	$0.23\lambda_g^2 \times 0.05\lambda_g$
[101]	4	12.0%	Y	S.A.	$0.76\lambda_g^2 \times 0.03\lambda_g$
[102]	10	4.0%	Y	S.A.	$1.92\lambda_g^2 \times 0.2\lambda_g$
[103]	10	32.9%	N	$\theta = -38^\circ$ to 40°	$6.4\lambda_g^2 \times 0.04\lambda_g$

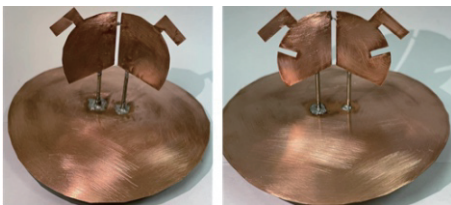


Figure 7 Prototypes of Pacman-shaped sectorial electric dipoles under multiple TE mode resonances.

When three resonant modes are excited and perturbed, the sectorial electric dipole may exhibit an octave radiation bandwidth [105]. More importantly, the sectorial electric

dipole can be employed to design dual-polarized antennas with port isolation as high as 35 dB owing to its superb polarization purity [104]. When a corner reflector is properly incorporated in front of a sectorial electric dipole under triple-mode resonance, the radiation dispersion can be finely tuned. In this sense, a backfire dipole antenna with nearly equal E-/H-planes and an inverse taper pattern can be implemented [106]: The antenna exhibits a stable, symmetric beam in the low- and moderate-frequency bands, and it exhibits an inverse taper pattern in the high-frequency band. Such characteristics are beneficial for compensation of edge illumination in a parabolic antenna system.

Selective sectorial electric dipole antennas are compared with their respective counterparts [107]–[110]. As tabulated in Table 5, the wideband sectorial dipole antennas can exhibit a performance superior or comparable to that of their counterparts with the fewest design parameters. More comprehensive comparisons have been presented in [104]–[106].

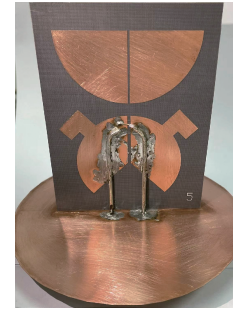
Table 5 Comparisons of wideband electrical dipole antennas

Ref.	Resonant modes	Number of design parameters	Impedance bandwidth
[104]	2	9	70.4%
[105]	3	13	73.3%
[107]	1	11	45.6%
[108]	1	17	45.0%
[109]	2	13	51.4%
[110]	3	31	52.7%

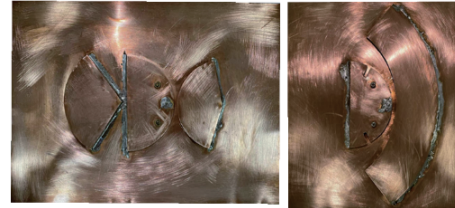
More recently, the mode synthesis design approach for 2-D, multimode resonant elementary antennas has also been extended to the design of directive antennas by incorporating one or more parasitic element(s). The sectorial electric dipole can be combined with either a 1-D linear dipole [111] or a 2-D sectorial dipole [112] to yield wideband Yagi-Uda antennas. Compared to the traditional Yagi-Uda antenna composed of 1-D, linear dipoles under single half-wavelength mode resonance, the multimode resonant Yagi-Uda antenna using a hybrid 1-D and 2-D dipole configuration may exhibit comparable or superior performance [111]. As illustrated in Figure 8(a), the size and angle of the director can be initially estimated by the mode synthesis approach and the multisource model [112] in an analytical manner. As a result, the antenna gain can be enhanced by 2 dB. The director is tightly coupled to the principal dipole at a small separation of 0.024 times the wavelength, which simultaneously yields a wide band and a compact size [112].

Similar to the 2-D sectorial electric Yagi-Uda antenna, MPAs with enhanced backfire/endfire gains can also be designed and implemented in a semi-analytical manner: As the initial design step, the mode synthesis chart can be employed to determine the first usable resonant mode, as well as the following usable counterparts under the gauged prototype dipole. Then, the multiple-point source model is employed to calculate the shape and position of the director(s) or reflector [113]–[115]. In this way, the basic configuration and the initial values of the key parameters can be basically set and analytically determined. Further numerical simulations may be carried out to tune and optimize the antenna performance as desired.

As a typical application, low-profile vehicular antennas under multiple high-order mode resonances can be implemented. Although only one director is incorporated into the dual-mode resonant principal dipole, the resultant backfire gain of triple-element designs can be enhanced to 4.2 dBi [113], at the cost of a high first sidelobe level of -5 dB.



(a)



(b)

Figure 8 Prototypes of directive multimode resonant antennas. (a) Yagi-Uda antenna using 2-D sectorial electric dipoles; and (b) Low-profile MPAs with enhanced backfire gain for vehicular applications.

Triple-mode resonance designs can be employed to suppress the first sidelobe level while maintaining the enhanced backfire or endfire gain [114], [115]: A circumferentially short-circuited, magnetic dipole with a radius of an odd-number multiple of the one-quarter wavelength can be incorporated into the triple-mode resonant principal MPA as a reflector. In this way, the backfire or endfire gains can be enhanced to 7.3 dBi (air substrate) and 4.1 dBi (Teflon substrate), respectively, without incorporating additional directors, and the first sidelobe level can be reduced to -15 dB and -9 dB, respectively.

The preceding paragraphs have comprehensively introduced the mode synthesis antenna design approach for the simplest 2-D multimode resonant antennas, i.e., the Pacman-shaped MPAs and the sectorial electric dipole antennas. As can be seen, the mode synthesis antenna approach is based on analytical theory. Antenna designers can use it to rapidly confirm the operational modes, quickly determine the basic configuration, and approximately estimate the initial values of the key antenna parameters. The mode synthesis process may be beneficial for clearly revealing the ultimate operation mechanism to antenna designers before they further perform a numerical simulation and optimization process. It provides powerful tools [29], [81], [82], [88]–[91] (mode synthesis charts and tables, multisource model, etc.) to antenna designers for a better understanding of and physical insights into multimode resonant antennas. In the mode synthesis antenna design approach, the “prototype dipole” analogously (not equivalently) serves as the “prototype low-pass filter” in the microwave filter synthesis approach, which can be employed to steer and manipulate the usable modes according to the parity of the eigenmodes.

Table 6 systematically compares the simplest, multimode resonant, Pacman-shaped antennas. As can be seen,

the mode synthesis design approach can yield high-gain, wide-beamwidth, CP, dual-polarized, and null frequency scanning antennas for wideband operations. For Pacman-shaped MPAs, the inherent low profile much less than 0.1 times the wavelength can be maintained [81], [82], [88]–[91]. Furthermore, the yielded antennas can be simply implemented on either an air substrate or printed circuit boards. Thus, the mode synthesis design approach has been validated to be independent of the material of the antenna substrate [29]. The mode synthesis antenna design approach is also well compatible with numerical design approaches: Numerical simulations can be purposefully performed based on the analytical, mode-synthesized results, with fewer endeavors and less overhead for numerically yielding the initial configuration. Hence, it can be concluded that the mode synthesis antenna design approach should be regarded as a semi-analytical approach with generality and robustness.

Table 6 Comparisons of the simplest, multimode resonant, 2-D Pacman-shaped antennas

Ref.	Number of resonant modes	Impedance bandwidth	Merit
[81]	2	14.5%	High gain
[82]	2	25.0%	Wide beamwidth
[90]	2	35.8%	Tilted CP and miniaturized patch
[91]	3	24.0%	Null frequency scanning
[104]	2	53.3%	Dual-polarized
[105]	3	73.3%	Octave bandwidth

IV. Discussion and Prospects

GO-EMT has been mathematically advanced to reveal the unbalance mechanism in antenna systems, and it has been employed to lay a foundation for the mode synthesis antenna design approach for multimode resonant antennas [29]. More recent developments and possible trends will be discussed and prospected in this section.

More recently, preliminary experimental studies on describing the performance of an unbalanced antenna system under multimode resonance have been performed [116], [117]: For an unbalanced coaxial cable, a new parameter called the “suppression rate of the unbalanced sheath current” may be defined [116]. In addition, the spurious radiations of the sheath current may be approximately estimated by the superposition of the multiple resonant high-order dipole modes excited in the feed line [117]. More rigorous analyses of unbalanced currents are still awaiting further investigation.

In addition to analysis and suppression of unbalanced currents, they can be transformed to provide a positive contribution to the antenna system. When the unbalanced currents are transformed, the antenna should operate in a “self-balanced” state [12], [118], [119]: For a Pacman-shaped magnetic dipole antenna, an additional stub can be incorporated into the angular bisector on the bottom layer. In this

way, the unbalanced currents on the bottom layer may be forced to flow on the stub, rather than excite the sheath of the feed line. Thus, the transformed electric currents and the magnetic current sheet on the aperture will superpose to yield a heart-shaped, broadened beam with a controllable beamwidth, and the antenna is automatically balanced without incorporating an external balun [12], [118]. This inspired the conceptual design of a “self-balanced magnetic dipole antenna” (SBMDA). In terms of the operational principle, the SBMDA can be reasonably treated as a “generalized complementary dipole antenna” under multimode resonance [29]: The transformed electric dipole and its copolarized, magnetic counterpart should co-dominate the unidirectional, heart-shaped radiation pattern similar to those of conventional complementary dipole antennas.

As theoretically formulated, the “unbalance degree” can be employed to tune the front-to-back ratio (FBR) of an SBMDA [118]: To attain the desired unbalance degree for high FBR (>30 dB) design, the shape of the stub can be accordingly modified. Similarly, the design approach can be extended to dual-band antennas [119]: A dual-mode resonant magnetic dipole can be stacked on an SBMDA, thus yielding a triple-mode resonant, dual-band, less frequency dispersive antenna with broadened E-plane patterns and a stable boresight gain of approximately 4 dBi in both bands. Selective SBMDA prototypes are shown in Figure 9(a)–(c).

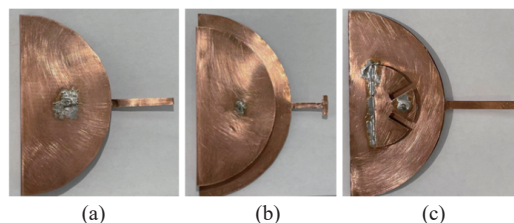


Figure 9 Prototypes of self-balanced magnetic dipole antennas. (a) Basic configuration; (b) Improved version with a high front-to-back ratio of over 30 dB; and (c) Stacked dual-band design with a broadened E-plane pattern and a less dispersive gain frequency response.

The relevant works on unbalanced current evaluation [116], [117] and SBMDAs [12], [118], [119] well validate that the unbalanced currents in an antenna system might not be simply treated as only “negative components”. If the unbalanced currents could be clearly identified and accurately estimated by GO-EMT [29], then they might be flexibly steered and reasonably utilized. Thus, it is earnestly expected that unbalanced currents can possibly serve as “new degrees of freedom in design” to yield more innovative elementary antennas and antenna systems in the future. More theoretical studies and engineering developments within the GO-EMT framework are still being explored.

For a theoretical framework with generality, the GO-EMT framework should be able to be flexibly extended to and be consistent with the frameworks of other antenna types such that a more universal unified framework is yielded, as illustrated in Figure 10. Recently, some endeavors have been made to extend the GO-EMT framework to

leaky-wave antennas by revealing the evolutionary relationship between multimode resonant annular sector MPAs and straight leaky-wave microstrip antennas [120]. The evolution between multimode antennas and leaky-wave antennas mathematically originates from the characteristic equation of the annular sector MPA: For an annular sector MPA with flare angle α , the inner radius ($\rho = a$) short-circuited and the outer radius ($\rho = b$) open-circuited, its characteristic equation can be readily expressed by (8a) [121].

$$\frac{J_\nu(ka)}{J'_\nu(ka)} = \frac{N_\nu(k\gamma a)}{N'_\nu(k\gamma a)}, \quad \gamma = \frac{b}{a}, \quad \nu = \frac{n\pi}{\alpha}, \quad n = 1, 2, \dots \quad (8a)$$

$$\frac{J_{\frac{1}{2}}(x)}{J'_{\frac{1}{2}}(x)} = \frac{N_{\frac{1}{2}}(x)}{N'_{\frac{1}{2}}(x)} \quad (8b)$$

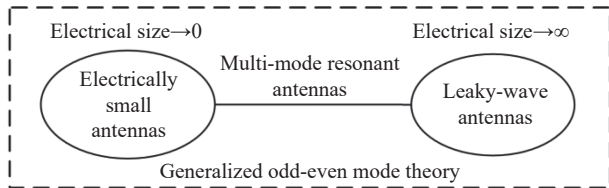


Figure 10 Generalized framework for multimode resonant antennas, leaky-wave antennas, and electrically small antennas.

Let the inner and outer radii simultaneously approach infinity [122] such that the annular sector evolves into a straight line and the flare angle $\alpha \rightarrow 2\pi$. Thus, (8a) may evolve into its limit case of (8b). The evolution process is illustrated in Figure 11(a). Solving (8a) and (8b), their eigenspectra are plotted in Figure 11(b). Intuitively, the finite case of (8a) ($\gamma = 3$, $\nu = 6/5$) may exhibit an oscillating eigenspectrum with discrete roots, while the limit case of (8b) may exhibit a nonoscillating, continuous eigenspectrum without discrete roots. A continuous spectrum should indicate the properties of nonresonant, leaky-wave antennas [123]. Thus, it can be evidently and mathematically concluded that the annular sector MPA could be evolved from a truncated, bent straight leaky-wave microstrip antenna [120].

In this sense, the mode synthesis antenna design approach can be employed to tune the resonant modes of the truncated leaky-wave antenna: The length of the prototype magnetic dipole can be employed to “truncate” the straight microstrip line and then “bend” it to the suitable angle α according to the mode gauge relation (7). Thus, the mathematical essence of and physical insights from the mode synthesis antenna design approach can be intuitively reflected in (7), (8) and Figure 11(b). As a result, the yielded multimode resonant annular sector MPA may naturally inherit the properties of a leaky-wave microstrip antenna to some extent: It may exhibit enhanced backfire or endfire gain in the direction parallel to the ground plane. Therefore, the design approach can be employed to implement low-profile antennas with a low elevation coverage ability. A fabricated prototype is shown in Figure 11(c). The work in [120]

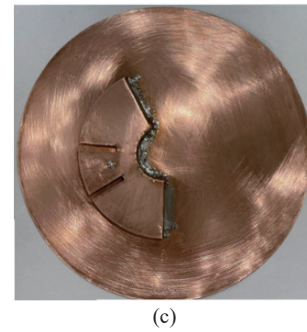
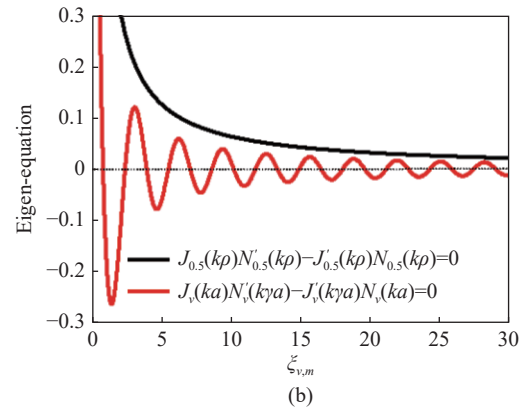
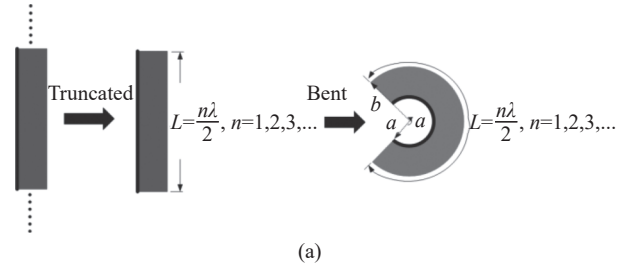


Figure 11 Evolution between a multimode resonant antenna and a leaky-wave antenna. (a) Conceptual illustration; (b) Spectrum of the characteristic equations; and (c) Prototype of a multimode resonant annular sector antenna evolved from a truncated, bent leaky-wave microstrip antenna.

paves a possible way to unify multimode resonant antennas and leaky-wave antennas. In the future, it would be a challenging but interesting task to disclose more crucial relationships between novel multimode antennas and leaky-wave antennas in a mathematical fashion with clear physical insights [120].

On the other hand, GO-EMT is also expected to be developed to be consistent with electrically small antennas. As has been investigated in [90], an asymmetric prototype dipole may yield a miniaturized patch size. The radius of a Pacman-shaped MPA can be naturally reduced to 0.18 times the wavelength, which is approaching the upper bound of “electrically small” of 0.159 times the wavelength [36], [124]. According to the mode synthesis table in [90] and [125], it has been validated that the radius can be reduced to less than 0.159 times the wavelength at the cost of single-mode resonant, narrowband operation [125]. Nevertheless, the spurious radiations from the unbalanced currents on the feed cable have not been fully suppressed by

using conventional balancing devices [125]. Once the unbalanced current can be fully suppressed, the mutual coupling effects (not only between the feed line and antenna but also between antenna elements) can be mitigated. As evidence, an annular sector patch antenna (port 1) has been co-located with a fully balanced sectorial dipole (port 2) to yield a dual-polarized probe antenna system that has been validated to exhibit a wide band, a superb high port isolation of over 50 dB [126], a low cross-polarization level and an effectively radiated, high boresight gain of up to 10.5 dBi, as plotted in Figure 12(a) to (d). Hence, for multimode resonant antennas, especially for electrically small antennas, balanced feeding always remains the most critical, tough problem [125], [126]. High performance balancing devices for electrically small antennas are desired, and it is expected that they could be developed within the GO-EMT theoretical framework in the future.

Moreover, PDE-based GO-EMT deduced in the context of “interior (waveguide) problems”, modal expansion approaches based on IEs and numerical techniques (i.e., MoM) have been intensively developed since the 1970s, such as the singularity expansion method (SEM) [127], the eigenmode expansion method (EEM) [128], the theory of characteristic modes (TCM) [129]–[132], and the theory of resonant modes (TRM) [133]. Attempts to unify the SEM, EEM, TCM and TRM have been made in [133], [134] in the context of the “exterior (scattering/radiation) problem”. It is also expected that PDE-based GO-EMT could be unified with the IE-based numerical modal expansion approaches to yield novel antenna design approaches with generality and robustness in the future.

The theoretical framework of GO-EMT and the mode synthesis antenna design approach have been systematically discussed and prospected. Ideally, similar to how mathematicians are curious as to how to “hear the shape of a drum” by using the eigenvalues (tones) and eigenfunctions (modes) [135], antenna designers hope to be able to predict the antenna shape in advance before initiating the numerical simulation and optimization process. With the aid of the mode synthesis antenna design approach, although antenna engineers can hardly “hear” the shape of an antenna, they can naturally design the simplest multimode resonant antennas [29]. In this sense, antenna engineers can tune and orchestrate multiple “tones” and “modes” as desired in a composer’s fashion to invent a series of elegant Pacman-shaped antennas with distinctive performance. Thus, GO-EMT reflects the symmetry, elegance and beauty of the mathematical nature, and the mode synthesis antenna design approach inspired by GO-EMT physically visualizes the multimode resonant electromagnetic fields.

V. Conclusion

On the basis of a more generalized, “multimode transmission, mode mismatching” premise, the author sought to deduce a simplified, semi-analytical theory by using spectral expansions of the odd- and even-symmetric eigenmode

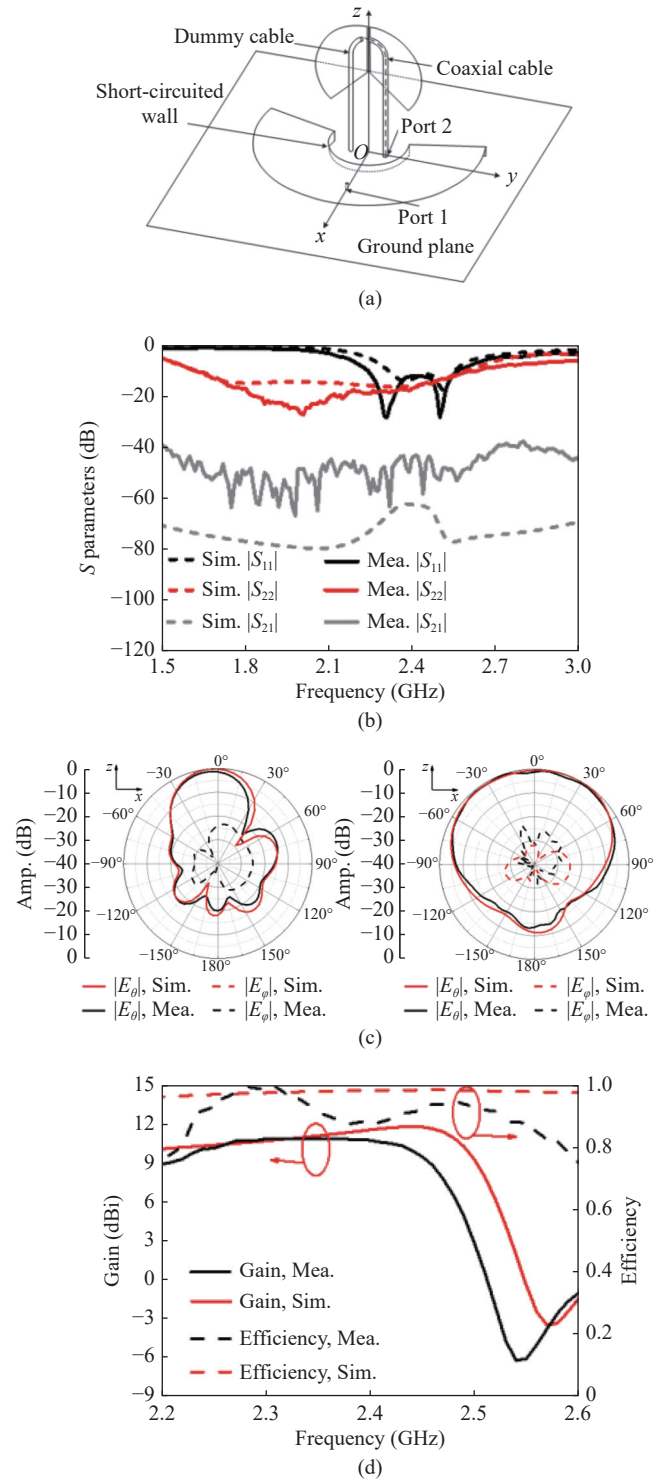


Figure 12 Measured and simulated results of a dual-polarized, balanced probe antenna system. (a) Schematic diagram of the antenna system; (b) Reflection coefficients and port isolations; (c) Normalized radiation patterns at port 1 and port 2 at 2.4 GHz; and (d) Gain and radiation efficiency at port 1.

functions, namely, “generalized odd-even mode theory (GO-EMT)”, to mathematically describe the mutual coupling effect between an antenna and a feed line. An approximate expression of the “unbalance degree” of the simplest, off-center-fed dipole antenna system has been derived. In

the context of the “interior problem”, GO-EMT should be a creative extension of classical waveguide theory [1]–[4], [31] with emphasis on modal parity mismatch. It provides clear physical understandings and qualitative design guidelines to antenna designers and inspires and motivates a semi-analytical mode synthesis antenna design approach for multimode resonant antennas. Under the guidance of GO-EMT, the multimode resonance mechanism can be intuitively understood, and simple closed-form formulas can be readily formulated to yield distinctive multimode resonant antennas. It is expected that GO-EMT could open a way for falsifying the 80-year old conclusion that “The discussion of coupled transmission lines and antennas has been nonmathematical because a complete analytical treatment of the difficult coupling problems is unavailable” [10], [29] in the future.

The newly developed GO-EMT is an approximate, deductive and extensible theory. It is compatible and consistent with the traditional antenna and transmission line theories [8]–[10]. However, it needs to be improved in both scientific and technical aspects. Scientifically, on the one hand, more mathematically rigorous formulations for accurately calculating the unbalance degree need to be deduced so that the theory could be extended to be mature and complete. On the other hand, motivated by the work revealing the evolution between multimode resonant and leaky-wave antennas [120], it would be an essentially fundamental, albeit extremely challenging, task to establish a unified theoretical framework for electrically small, multimode resonant and leaky-wave antennas. Technically, many possible works to suppress or utilize the unbalanced currents in complicated antenna systems could be performed, some of which may include (but are not limited to) the following: i) Applications of unbalanced currents: In a complex antenna system, unbalanced currents can possibly be employed as more new degrees of freedom in design, according to the modal parity matching state between the antenna and feed line. ii) Development of novel balancing devices (i.e., baluns): To compensate for the modal parity mismatch between the feed line and antenna in a “field” fashion, new balancing device configurations as simple as possible can be implemented based on GO-EMT and the semi-analytical design approach with the aid of numerical simulations.

The GO-EMT-inspired, semi-analytical mode synthesis antenna design approach can provide the necessary mathematical understanding of and intuitive physical insights into multimode resonant antennas. It is compatible with other wideband antenna design approaches based on numerical techniques [50], [131], [133], [136]. Although it is independent of the antenna substrate material, it is compatible with advanced materials and fabrication technologies, which may inspire more innovative multimode resonant antennas and antenna systems in the future.

Acknowledgements

This work is supported by the National Key Research and

Development Program of China (Grant No. 2021YFE0205 900) and the Key Technologies R&D Program of Jiangsu (Prospective and Key Technologies for Industry) (Grant Nos. BE2022067 and BE2022067-2). The author is indebted to Prof. Ming Zhang, Nanjing University of Posts and Telecommunications, for his kind discussions, encouragement and beneficial suggestions regarding this article. The author would also like to thank his Ph.D. and M.S. students, Ms. Xiao-Hui MAO, Ms. Fei-Yan JI, and Ms. Xiao-Yu SONG, for their kind assistance in editing the figures of this article.

References

- [1] L. Rayleigh, “On the passage of electric waves through tubes, or the vibration of dielectric cylinders,” *Philosophical Magazine*, vol. 43, no. 261, pp. 125–131, 1897.
- [2] D. Hondros and P. Debye, “Elektromagnetische wellen an dielektrischen drähten,” *Annalen der Physik*, vol. 337, no. 8, pp. 465–476, 1910.
- [3] W. L. Barrow, “Transmission of electromagnetic waves in hollow tubes of metal,” *Proceedings of the Institute of Radio Engineers*, vol. 24, no. 10, pp. 1298–1328, 1936.
- [4] J. R. Carson, S. P. Mead, and S. A. Schelkunoff, “Hyper-frequency wave guides—mathematical theory,” *The Bell System Technical Journal*, vol. 15, no. 2, pp. 310–333, 1936.
- [5] P. R. Garabedian, “An integral equation governing electromagnetic waves,” *Quarterly of Applied Mathematics*, vol. 12, no. 4, pp. 428–433, 1955.
- [6] S. A. Schelkunoff, “Transmission theory of plane electromagnetic waves,” *Proceedings of the Institute of Radio Engineers*, vol. 25, no. 11, pp. 1457–1492, 1937.
- [7] S. A. Schelkunoff and H. T. Friis, *Antennas: Theory and Practice*. John Wiley & Sons, New York, NY, USA, 1952.
- [8] S. A. Schelkunoff, “Generalized telegraphist's equations for waveguides,” *The Bell System Technical Journal*, vol. 31, no. 4, pp. 784–801, 1952.
- [9] S. A. Schelkunoff, “Conversion of Maxwell's equations into generalized telegraphist's equations,” *The Bell System Technical Journal*, vol. 34, no. 5, pp. 995–1043, 1955.
- [10] R. King, “Coupled antennas and transmission lines,” *Proceedings of the IRE*, vol. 31, no. 11, pp. 626–640, 1943.
- [11] S. Silver, *Microwave Antenna Theory and Design*. McGraw-Hill Book Co., New York, NY, USA, pp. 242–248, 1949.
- [12] C. Shen, W. J. Lu, and L. Zhu, “Planar self-balanced magnetic dipole antenna with wide beamwidth characteristic,” *IEEE Transactions on Antennas and Propagation*, vol. 67, no. 7, pp. 4860–4865, 2019.
- [13] S. H. Hu, “The Balun family,” *Microwave Journal*, vol. 30, no. 9, pp. 227–229, 1987.
- [14] S. H. Hu, *Practical Radio Frequency Technologies*. Publishing House of Electronics Industry, Beijing, pp. 54–70, 2004. (in Chinese)
- [15] E. C. Cecil and P. J. Lade, “Wireless aerial system,” *Patent*, 2167709, US, 1939-08-01.
- [16] J. W. Duncan and V. P. Minerva, “100: 1 bandwidth Balun transformer,” *Proceedings of the IRE*, vol. 48, no. 2, pp. 156–164, 1960.
- [17] H. R. Phelan, “A wide-band parallel-connected balun,” *IEEE Transactions on Microwave Theory and Techniques*, vol. 18, no. 5, pp. 259–263, 1970.
- [18] J. Andersen and H. Rasmussen, “Decoupling and descattering networks for antennas,” *IEEE Transactions on Antennas and Propagation*, vol. 24, no. 6, pp. 841–846, 1976.
- [19] D. Campbell, S. Fich, and F. Schwering, “Suppression of parasitic currents on feed lines of colinear dual antenna systems,” *IEEE*

- Transactions on Antennas and Propagation*, vol. 28, no. 5, pp. 658–662, 1980.
- [20] M. J. Slater and J. T. Bernhard, “Study of Balun effects with electrically small antennas for a whitespace direction finding system,” in *Proceedings of 2010 IEEE Antennas and Propagation Society International Symposium*, Toronto, ON, Canada, pp. 1–4, 2010.
- [21] T. Fukasawa, N. Yoneda, and H. Miyashita, “Investigation on current reduction effects of Baluns for measurement of a small antenna,” *IEEE Transactions on Antennas and Propagation*, vol. 67, no. 7, pp. 4323–4329, 2019.
- [22] W. Kelvin, “The radiation field of an unbalanced dipole,” *Proceedings of the IRE*, vol. 34, no. 7, pp. 440–444, 1946.
- [23] E. A. Blasi, “The theory and application of the radiation mutual-coupling factor,” *Proceedings of the IRE*, vol. 42, no. 7, pp. 1179–1183, 1954.
- [24] K. Iizuka and R. King, “The effect of an unbalance on the current along a dipole antenna,” *IRE Transactions on Antennas and Propagation*, vol. 10, no. 6, pp. 702–707, 1962.
- [25] T. Watanabe, O. Wada, T. Miyashita, *et al.*, “Common-mode-current generation caused by difference of unbalance of transmission lines on a printed circuit board with narrow ground pattern,” *IEICE Transactions on Communications*, vol. E83-B, no. 3, pp. 593–599, 2000.
- [26] S. Hamada, T. Kawashima, J. Ochura, *et al.*, “Influence of balance-unbalance conversion factor on radiated emission characteristics of balanced cables,” in *Proceedings of 2001 IEEE EMC International Symposium. Symposium Record. International Symposium on Electromagnetic Compatibility*, Montreal, QC, Canada, pp. 31–36, 2001.
- [27] J. S. McLean, “Balancing networks for symmetric antennas. I. Classification and fundamental operation,” *IEEE Transactions on Electromagnetic Compatibility*, vol. 44, no. 4, pp. 503–514, 2002.
- [28] J. S. McLean, “Balancing networks for symmetric antennas: Part II—Practical implementation and modeling,” *IEEE Transactions on Electromagnetic Compatibility*, vol. 46, no. 1, pp. 24–32, 2004.
- [29] W. J. Lu and L. Zhu, *Multi-Mode Resonant Antennas: Theory, Design, and Applications*. CRC Press, Boca Raton, FL, USA, pp. 1–25, 2022.
- [30] W. J. Lu, X. H. Mao, and F. Y. Ji, “Generalized odd-even mode theory: A unified theoretical framework of multi-mode resonant antennas,” in *Proceedings of 2023 National Conference of Antenna*, Harbin, China, pp. 2127–2129, 2023. (in Chinese)
- [31] R. E. Collin, *Field Theory of Guided Waves*, 2nd ed. , IEEE Press, New York, NY, USA, pp. 55–102, 1991.
- [32] W. X. Zhang, *Partial Differential Equations in Radio Techniques*. Publishing House of National Defense Industry, Beijing, pp. 254–291, 1982. (in Chinese)
- [33] M. Leontovich and M. Levin, “Towards a theory on the simulation of the oscillations in dipole antennas,” *Zhurnal Tekhnicheskoi Fiziki*, vol. 14, no. 9, pp. 487–506, 1944. (in Russian)
- [34] W. J. Lu, J. Yu, and L. Zhu, “On the multi-resonant antennas: Theory, history, and new development,” *International Journal of RF and Microwave Computer-Aided Engineering*, vol. 29, no. 9, article no. e21808, 2019.
- [35] J. Xu, W. J. Lu, X. T. Wu, *et al.*, “Novel offset-fed dual-band aperture-dipole composite antenna: Operating principle and design approach,” *International Journal of RF and Microwave Computer-Aided Engineering*, vol. 25, no. 5, pp. 382–393, 2015.
- [36] H. Schantz, *The Art and Science of Ultrawideband Antennas*, 2nd ed. , Artech House, Boston, MA, USA, pp. 176–181, 435–437, 2015.
- [37] J. V. N. Granger and J. T. Bolljahn, “Aircraft antennas,” *Proceedings of the IRE*, vol. 43, no. 5, pp. 533–550, 1955.
- [38] W. J. Lu and L. Zhu, “Wideband stub-loaded slotline antennas under multi-mode resonance operation,” *IEEE Transactions on Antennas and Propagation*, vol. 63, no. 2, pp. 818–823, 2015.
- [39] W. J. Lu and L. Zhu, “A novel wideband slotline antenna with dual resonances: Principle and design approach,” *IEEE Antennas and Wireless Propagation Letters*, vol. 14, pp. 795–798, 2015.
- [40] W. J. Lu and L. Zhu, “Planar dual-mode wideband antenna using short-circuited-strips loaded slotline radiator: Operation principle, design, and validation,” *International Journal of RF and Microwave Computer-Aided Engineering*, vol. 25, no. 7, pp. 573–581, 2015.
- [41] C. R. Guo, W. J. Lu, Z. S. Zhang, *et al.*, “Wideband non-traveling-wave triple-mode slotline antenna,” *IET Microwaves, Antennas & Propagation*, vol. 11, no. 6, pp. 886–891, 2017.
- [42] S. G. Wang, W. J. Lu, C. R. Guo, *et al.*, “Wideband slotline antenna with frequency-spatial steerable notch-band in radiation gain,” *Electronics Letters*, vol. 53, no. 10, pp. 650–652, 2017.
- [43] G. E. Ponchak, “Slotline switch based on a lattice circuit,” *IEEE Microwave and Wireless Components Letters*, vol. 26, no. 1, pp. 43–45, 2016.
- [44] L. Pazin and Y. Leviatan, “On the matching characteristics of a rectangular slot located near the edge of a finite-size ground plane,” *Journal of Electromagnetic Waves and Applications*, vol. 30, no. 5, pp. 579–588, 2016.
- [45] D. L. Wen and Y. Hao, “A wideband T-shaped slot antenna and its MIMO application,” in *Proceedings of 2016 IEEE International Symposium on Antennas and Propagation*, Fajardo, PR, USA, pp. 1761–1762, 2016.
- [46] H. Y. Wang, D. W. Zhou, L. Xue, *et al.*, “Modal analysis and excitation of wideband slot antennas,” *IET Microwaves, Antennas & Propagation*, vol. 11, no. 13, pp. 1887–1891, 2017.
- [47] M. A. C. Niamien, “Spectral domain-based input impedance prediction of a CPW-fed notch antenna,” *IEEE Antennas and Wireless Propagation Letters*, vol. 18, no. 1, pp. 133–137, 2019.
- [48] C. Wang, H. Y. Wang, P. F. Wu, *et al.*, “Dual-band closed-slot MIMO antenna for terminal wireless applications,” *IEEE Transactions on Antennas and Propagation*, vol. 70, no. 8, pp. 6514–6525, 2022.
- [49] D. G. Seo, J. H. Kim, S. H. Ahn, *et al.*, “A 915 MHz dual polarized meandered dipole antenna with dual resonance,” in *Proceedings of 2018 International Symposium on Antennas and Propagation*, Busan, Korea, pp. 1–2, 2018.
- [50] N. M. Mohamed-Hicho, E. Antonino-Daviu, M. Cabedo-Fabrés, *et al.*, “Designing slot antennas in finite platforms using characteristic modes,” *IEEE Access*, vol. 6, pp. 41346–41355, 2018.
- [51] Y. Luo, Z. N. Chen, and K. M. Ma, “Enhanced bandwidth and directivity of a dual-mode compressed high-order mode stub-loaded dipole using characteristic mode analysis,” *IEEE Transactions on Antennas and Propagation*, vol. 67, no. 3, pp. 1922–1925, 2019.
- [52] S. Ahirwar, A. P. Rao, and M. Chakravarthy, “Design of a broadband mode compressed high gain dipole antenna with artificial magnetic conductor as a reflector,” *Sādhanā*, vol. 48, no. 3, 2023.
- [53] R. Solanki, “Third- and fifth-order mode compression of a dipole antenna,” *IEEE Transactions on Antennas and Propagation*, vol. 70, no. 12, pp. 12294–12298, 2022.
- [54] W. J. Lu, L. Zhu, K. W. Tam, *et al.*, “Wideband dipole antenna using multi-mode resonance concept,” *International Journal of Microwave and Wireless Technologies*, vol. 9, no. 2, pp. 365–371, 2017.
- [55] D. S. Zhang, S. S. Gu, M. G. Pan, *et al.*, “Hybrid lumped-distributed loading design approach to wideband dual-mode resonant monopole antennas,” *International Journal of RF and Microwave Computer-Aided Engineering*, vol. 32, no. 11, article no. e23369, 2022.
- [56] C. A. Nickle, R. B. Dome, and W. W. Brown, “Control of radiating properties of antennas,” *Proceedings of the Institute of Radio Engineers*, vol. 22, no. 12, pp. 1362–1373, 1934.
- [57] S. A. Adekola, T. C. Erinosh, and K. A. Amusa, “Resonant half-wave dipole and its odd integral multiples,” in *Proceedings of 2019 Photonics & Electromagnetics Research Symposium - Spring*, Rome, Italy, pp. 1405–1412, 2019.
- [58] A. N. Yeganeh, A. Mahan, S. H. Sedighy, *et al.*, “Design of a new compact planar wide band dipole antenna,” *Microwave and Opti-*

- cal Technology Letters*, vol. 59, no. 12, pp. 3189–3197, 2017.
- [59] H. Shin, S. Jiang, J. Yang, *et al.*, “A new ultra-wideband miniaturized antenna with a double-branch radiator,” *Microwave and Optical Technology Letters*, vol. 62, no. 5, pp. 2085–2089, 2020.
- [60] S. Wang, J. Park, H. Shim, *et al.*, “Design of a wideband coupled feed dipole antenna for PCL array systems,” *Journal of Electrical Engineering & Technology*, vol. 15, no. 5, pp. 2251–2258, 2020.
- [61] J. S. Tong, J. Y. Guo, J. J. Huo, *et al.*, “A compact nonsymmetric wideband dipole antenna for borehole radar application,” *IEEE Transactions on Antennas and Propagation*, vol. 69, no. 8, pp. 4323–4331, 2021.
- [62] M. A. Abdalla, M. El Atrash, A. A. A. Aziz, *et al.*, “A compact dual-band D-CRLH-based antenna with self-isolation functionality,” *International Journal of Microwave and Wireless Technologies*, vol. 14, no. 5, pp. 616–625, 2022.
- [63] B. Xiao, H. Wong, M. Li, *et al.*, “Dipole antenna with both odd and even modes excited and tuned,” *IEEE Transactions on Antennas and Propagation*, vol. 70, no. 3, pp. 1643–1652, 2022.
- [64] W. C. Yang, Y. Z. Li, Q. Xue, *et al.*, “Miniaturized broadband dual-polarized dipole antenna based on multiple resonances and its array for base-station applications,” *IEEE Transactions on Antennas and Propagation*, vol. 70, no. 11, pp. 11188–11193, 2022.
- [65] Y. Chen, W. J. Lu, L. Zhu, *et al.*, “Square loop antenna under even-mode operation: Modelling, validation and implementation,” *International Journal of Electronics*, vol. 104, no. 2, pp. 271–285, 2017.
- [66] C. Y. Yuan, W. J. Lu, C. Gao, *et al.*, “Balanced circularly polarized square loop antenna under even-mode resonance,” *International Journal of RF and Microwave Computer-Aided Engineering*, vol. 28, no. 6, article no. e21280, 2018.
- [67] L. Xu, W. J. Lu, C. Y. Yuan, *et al.*, “Dual circularly polarized loop antenna using a pair of resonant even-modes,” *International Journal of RF and Microwave Computer-Aided Engineering*, vol. 29, no. 6, article no. e21703, 2019.
- [68] J. Y. Wang, W. J. Lu, W. L. Zhang, *et al.*, “Balanced low-profile wide beamwidth circularly polarized stacked loop antenna,” *International Journal of RF and Microwave Computer-Aided Engineering*, vol. 31, no. 11, article no. e22848, 2021.
- [69] L. Zhu, S. Sun, and W. Menzel, “Ultra-wideband (UWB) band-pass filters using multiple-mode resonator,” *IEEE Microwave and Wireless Components Letters*, vol. 15, no. 11, pp. 796–798, 2005.
- [70] J. D. Kraus, “Helical beam antennas for wide-band applications,” *Proceedings of the IRE*, vol. 36, no. 10, pp. 1236–1242, 1948.
- [71] G. Deschamps and P. Mast, “Poincaré sphere representation of partially polarized fields,” *IEEE Transactions on Antennas and Propagation*, vol. 21, no. 4, pp. 474–478, 1973.
- [72] T. Fujimoto and C. E. Guan, “A compact printed hybrid-mode antenna for dual-band dual-sense circular polarisation,” *IET Microwaves, Antennas & Propagation*, vol. 17, no. 10, pp. 777–785, 2023.
- [73] S. Chaudhuri, R. S. Kshetrimayum, and R. K. Sonkar, “High interport isolation dual circularly polarized slot antenna with interdigital capacitor,” *International Journal of RF and Microwave Computer-Aided Engineering*, vol. 29, no. 10, article no. e21903, 2019.
- [74] X. X. Ding, S. N. Wu, Z. Q. Zhao, *et al.*, “Meta-surface loading broadband and high-aperture efficiency dual circularly polarized patch antenna,” *International Journal of RF and Microwave Computer-Aided Engineering*, vol. 31, no. 3, article no. e22525, 2021.
- [75] C. N. Liu, C. Y. Yuan, W. J. Lu, *et al.*, “Conceptual design of wideband balanced circularly polarized dual-loop antenna,” in *Proceedings of 2018 International Workshop on Antenna Technology*, Nanjing, China, pp. 1–3, 2018.
- [76] D. D. Wang, C. Y. Yuan, W. J. Lu, *et al.*, “Conceptual design of a dual-band circularly polarized square loop antenna under even-mode resonance,” in *Proceedings of 2017 Sixth Asia-Pacific Conference on Antennas and Propagation*, Xi’an, China, pp. 1–3, 2017.
- [77] W. L. Zhang, D. D. Wang, L. Xu, *et al.*, “Improved design of a dual-band circularly polarized square loop antenna under even-mode resonance,” in *Proceedings of 2019 International Conference on Microwave and Millimeter Wave Technology*, Guangzhou, China, pp. 1–3, 2019.
- [78] X. Wang, H. Zhang, Z. Tian, *et al.*, “Miniaturized Poincaré sphere source antenna loaded by a pair of lumped inductors,” in *Proceedings of 2023 International Conference on Microwave and Millimeter Wave Technology*, Qingdao, China, pp. 1–3, 2023.
- [79] H. Matzner and E. Levine, “Can $\lambda/4$ radiators be really isotropic?” *International Journal of Antennas and Propagation*, vol. 2012, article no. 187123, 2012.
- [80] Q. Li, W. J. Lu, S. G. Wang, *et al.*, “Planar quasi-isotropic magnetic dipole antenna using fractional-order circular sector cavity resonant mode,” *IEEE Access*, vol. 5, pp. 8515–8525, 2017.
- [81] W. J. Lu, Q. Li, S. G. Wang, *et al.*, “Design approach to a novel dual-mode wideband circular sector patch antenna,” *IEEE Transactions on Antennas and Propagation*, vol. 65, no. 10, pp. 4980–4990, 2017.
- [82] W. J. Lu, X. Q. Li, Q. Li, *et al.*, “Generalized design approach to compact wideband multi-resonant patch antennas,” *International Journal of RF and Microwave Computer-Aided Engineering*, vol. 28, no. 8, article no. e21481, 2018.
- [83] J. B. Keller and S. I. Rubinow, “Asymptotic solution of eigenvalue problems,” *Annals of Physics*, vol. 9, no. 81, pp. 24–75, 1960.
- [84] R. H. T. Bates and F. L. Ng, “Point matching computation of transverse resonances,” *International Journal for Numerical Methods in Engineering*, vol. 6, no. 2, pp. 155–168, 1973.
- [85] J. R. Kuttler and V. G. Sigillito, “Eigenvalues of the Laplacian in two dimensions,” *SIAM Review*, vol. 26, no. 2, pp. 163–193, 1984.
- [86] P. A. Laura, “On the determination of the natural frequency of a star-shaped membrane,” *The Journal of the Royal Aeronautical Society*, vol. 68, no. 640, pp. 274–275, 1964.
- [87] J. Yu and W. J. Lu, “Design approach to dual-resonant, very low-profile circular sector patch antennas,” in *Proceedings of 2019 International Conference on Microwave and Millimeter Wave Technology*, Guangzhou, China, pp. 1–3, 2019.
- [88] X. H. Mao, F. Y. Ji, S. S. Gu, *et al.*, “Circumferentially short-circuited circular sector patch antenna with broadened beamwidth,” in *Proceedings of 2021 IEEE International Symposium on Antennas and Propagation and USNC-URSI Radio Science Meeting*, Singapore, Singapore, pp. 1397–1398, 2021.
- [89] X. H. Mao, W. J. Lu, F. Y. Ji, *et al.*, “Dual radial-resonant wide beamwidth circular sector microstrip patch antennas,” *Chinese Journal of Electronics*, vol. 32, no. 4, pp. 710–719, 2023.
- [90] J. Yu, W. J. Lu, Y. Cheng, *et al.*, “Tilted circularly polarized beam microstrip antenna with miniaturized circular sector patch under wideband dual-mode resonance,” *IEEE Transactions on Antennas and Propagation*, vol. 68, no. 9, pp. 6580–6590, 2020.
- [91] Z. F. Wu, W. J. Lu, J. Yu, *et al.*, “Wideband null frequency scanning circular sector patch antenna under triple resonance,” *IEEE Transactions on Antennas and Propagation*, vol. 68, no. 11, pp. 7266–7274, 2020.
- [92] Z. F. Wu, J. Yu, and W. J. Lu, “Investigations of multi-resonant wideband null frequency scanning microstrip patch antennas,” in *Proceedings of 2020 IEEE Asia-Pacific Microwave Conference*, Hong Kong, China, pp. 179–181, 2020.
- [93] X. H. Mao, W. J. Lu, F. Y. Ji, *et al.*, “Triple-mode resonant null frequency scanning antenna with positive scanned slope,” *International Journal of RF and Microwave Computer-Aided Engineering*, vol. 32, no. 10, article no. e23313, 2022.
- [94] C. L. Chen, “A single-layer single-patch dual-polarized high-gain cross-shaped microstrip patch antenna,” *IEEE Antennas and Wireless Propagation Letters*, vol. 22, no. 10, pp. 2417–2421, 2023.
- [95] X. Zhang and L. Zhu, “Gain-enhanced patch antennas with loading of shorting pins,” *IEEE Transactions on Antennas and Propagation*, vol. 64, no. 8, pp. 3310–3318, 2016.
- [96] A. Afshani and K. Wu, “Dual-polarized patch antenna excited concurrently by a dual-mode substrate integrated waveguide,” *IEEE*

- Transactions on Antennas and Propagation*, vol. 70, no. 3, pp. 2322–2327, 2022.
- [97] Y. W. Hou, Z. J. Shao, Y. P. Zhang, *et al.*, “A wideband differentially fed dual-polarized laminated resonator antenna,” *IEEE Transactions on Antennas and Propagation*, vol. 69, no. 7, pp. 4148–4153, 2021.
- [98] Y. Zhang, Z. L. Xue, and W. Hong, “Planar substrate-integrated endfire antenna with wide beamwidth for Q-band applications,” *IEEE Antennas and Wireless Propagation Letters*, vol. 16, pp. 1990–1993, 2017.
- [99] Y. J. He and Y. Li, “Dual-polarized microstrip antennas with capacitive via fence for wide beamwidth and high isolation,” *IEEE Transactions on Antennas and Propagation*, vol. 68, no. 7, pp. 5095–5103, 2020.
- [100] W. B. Qiu, C. Chen, W. D. Chen, *et al.*, “A planar dipole antenna with parasitic elements for beamwidth enhancement across a wide frequency band,” in *Proceedings of 2017 IEEE International Symposium on Antennas and Propagation & USNC/URSI National Radio Science Meeting*, San Diego, CA, USA, pp. 333–334, 2017.
- [101] F. A. Dicandia, S. Genovesi, and A. Monorchio, “Null-steering antenna design using phase-shifted characteristic modes,” *IEEE Transactions on Antennas and Propagation*, vol. 64, no. 7, pp. 2698–2706, 2016.
- [102] J. Tamura and H. Arai, “Compact null steering antenna with two parasitic elements for angle-of-arrival estimation,” *IEEE Antennas and Wireless Propagation Letters*, vol. 19, no. 7, pp. 1123–1126, 2020.
- [103] M. F. Huang and J. H. Liu, “A null frequency scanning leaky-wave antenna,” *IEEE Transactions on Antennas and Propagation*, vol. 70, no. 9, pp. 7625–7635, 2022.
- [104] Z. B. Zhao, W. J. Lu, L. Zhu, *et al.*, “Wideband wide beamwidth full-wavelength sectorial dipole antenna under dual-mode resonance,” *IEEE Transactions on Antennas and Propagation*, vol. 69, no. 1, pp. 14–24, 2021.
- [105] C. X. Pan, W. J. Lu, W. Q. Jia, *et al.*, “Triple-resonant wideband 1.5-wavelength sectorial dipole antenna,” *International Journal of RF and Microwave Computer-Aided Engineering*, vol. 31, no. 8, article no. e22728, 2021.
- [106] Y. Xiao, W. J. Lu, M. L. Zhao, *et al.*, “Triple-mode resonant backfire feed antenna with nearly equal E/H-plane and inverse taper patterns,” *IEEE Transactions on Circuits and Systems II: Express Briefs*, vol. 70, no. 6, pp. 1946–1950, 2023.
- [107] L. Ge and K. M. Luk, “A magneto-electric dipole antenna with low-profile and simple structure,” *IEEE Antennas and Wireless Propagation Letters*, vol. 12, pp. 140–142, 2013.
- [108] Y. H. Cui, X. N. Gao, and R. L. Li, “A broadband differentially fed dual-polarized planar antenna,” *IEEE Transactions on Antennas and Propagation*, vol. 65, no. 6, pp. 3231–3234, 2017.
- [109] H. Li and Y. Li, “Mode compression method for wideband dipole antenna by dual-point capacitive loadings,” *IEEE Transactions on Antennas and Propagation*, vol. 68, no. 8, pp. 6424–6428, 2020.
- [110] W. X. An, X. Wang, H. P. Fu, *et al.*, “Low-profile wideband slot-loaded patch antenna with multiresonant modes,” *IEEE Antennas and Wireless Propagation Letters*, vol. 17, no. 7, pp. 1309–1313, 2018.
- [111] W. Q. Jia and W. J. Lu, “Dual-resonant wideband Yagi-Uda antennas using full-wavelength sectorial dipole,” in *Proceedings of 2021 International Conference on Microwave and Millimeter Wave Technology*, Nanjing, China, pp. 1–3, 2021.
- [112] W. Q. Jia, F. Y. Ji, W. J. Lu, *et al.*, “Dual-resonant high-gain wideband Yagi-Uda antenna using full-wavelength sectorial dipoles,” *IEEE Open Journal of Antennas and Propagation*, vol. 2, pp. 872–881, 2021.
- [113] X. Q. Xing, W. J. Lu, F. Y. Ji, *et al.*, “Low-profile dual-resonant wideband backfire antenna for vehicle-to-everything applications,” *IEEE Transactions on Vehicular Technology*, vol. 71, no. 8, pp. 8330–8340, 2022.
- [114] M. L. Zhao, F. Y. Ji, W. J. Lu, *et al.*, “Backfire patch antenna with enhanced gain and low side-lobe level under triple-mode resonance,” *International Journal of RF and Microwave Computer-Aided Engineering*, vol. 2023, article no. 9639026, 2023.
- [115] M. L. Zhao, X. Q. Xing, Y. Xiao, *et al.*, “Triple-mode resonant planar antenna with enhanced endfire radiation,” in *Proceedings of 2022 International Applied Computational Electromagnetics Society Symposium*, Xuzhou, China, pp. 1–2, 2022.
- [116] M. G. Pan, L. Liu, Z. B. Zhao, *et al.*, “Preliminary study on suppression rate of unbalanced sheath current of coaxial cable using sleeve choke,” in *Proceedings of 2022 International Conference on Microwave and Millimeter Wave Technology*, Harbin, China, pp. 1–3, 2022.
- [117] M. G. Pan, D. S. Zhang, L. Liu, *et al.*, “Unbalanced cable effect on planar quasi-isotropic magnetic dipole antennas,” *Journal of Nanjing University of Posts and Telecommunications (Natural Science Edition)*, vol. 42, no. 4, pp. 64–68, 2022. (in Chinese)
- [118] H. Wu, W. J. Lu, C. Shen, *et al.*, “Wide beamwidth planar self-balanced magnetic dipole antenna with enhanced front-to-back ratio,” *International Journal of RF and Microwave Computer-Aided Engineering*, vol. 30, no. 5, article no. e22171, 2020.
- [119] S. J. Li, W. J. Lu, and L. Zhu, “Dual-band stacked patch antenna with wide E-plane beam width and stable gain at both bands,” *Microwave and Optical Technology Letters*, vol. 63, no. 4, pp. 1264–1270, 2021.
- [120] J. Yu, W. J. Lu, Y. Cheng, *et al.*, “Dual-resonant wideband microstrip annular sector patch antenna with increased backfire radiations,” *IEEE Transactions on Antennas and Propagation*, vol. 70, no. 6, pp. 4181–4188, 2022.
- [121] R. Garg, P. Bhartia, I. Bahl, *et al.*, *Microstrip Antenna Design Handbook*. Artech House, Boston, MA, USA, pp. 387–388, 2001.
- [122] R. Courant and D. Hilbert, *Methods of Mathematical Physics*. M. Qian, trans, Science Press, Beijing, 1958. (in Chinese)
- [123] N. Marcuvitz, “On field representations in terms of leaky modes or eigenmodes,” *IRE Transactions on Antennas and Propagation*, vol. 4, no. 3, pp. 192–194, 1956.
- [124] L. J. Chu, “Physical limitations of omni-directional antennas,” *Journal of Applied Physics*, vol. 19, no. 12, pp. 1163–1175, 1948.
- [125] J. Yu and W. J. Lü, “Electrically small quasi-isotropic circular sector magnetic dipole antenna,” *Acta Electronica Sinica*, vol. 51, no. 8, pp. 2003–2010, 2023. (in Chinese)
- [126] W. J. Lu, X. Y. Song, J. P. Zong, *et al.*, “A dual-polarized probe antenna and its design approach,” *Patent*, 202310449827. X, CN, 2023-07-14. (in Chinese)
- [127] C. E. Baum, “On the singularity expansion method for the solution of electromagnetic interaction problems,” *Kirtland Air Force Base, Interaction Note*, No. 88, 1971.
- [128] C. E. Baum, “On the eigenmode expansion method for electromagnetic scattering and antenna problems part II: Asymptotic expansion of eigenmode-expansion parameters in the complex-frequency plane,” *Air Force Weapons Laboratory, Interaction Note*, IN 472, 1988.
- [129] R. Harrington and J. Mautz, “Theory of characteristic modes for conducting bodies,” *IEEE Transactions on Antennas and Propagation*, vol. 19, no. 5, pp. 622–628, 1971.
- [130] R. Harrington and J. Mautz, “Computation of characteristic modes for conducting bodies,” *IEEE Transactions on Antennas and Propagation*, vol. 19, no. 5, pp. 629–639, 1971.
- [131] B. K. Lau, M. Capek, and A. M. Hassan, “Characteristic modes: Progress, overview, and emerging topics,” *IEEE Antennas and Propagation Magazine*, vol. 64, no. 2, pp. 14–22, 2022.
- [132] M. Capek and K. Schab, “Computational aspects of characteristic mode decomposition: An overview,” *IEEE Antennas and Propagation Magazine*, vol. 64, no. 2, pp. 23–31, 2022.
- [133] R. Q. Xiao, W. Geyi, and W. Wu, “Theory of resonant modes and its application,” *IEEE Access*, vol. 9, pp. 114945–114956, 2021.
- [134] S. D. Huang, J. Pan, and Y. Y. Luo, “Study on the relationships between eigenmodes, natural modes, and characteristic modes of perfectly electric conducting bodies,” *International Journal of Antennas and Propagation*, vol. 2018, article no. 8735635, 2018.

- [135] M. Kac, "Can one hear the shape of a drum?," *The American Mathematical Monthly*, vol. 73, no. 4, pp. 1–23, 1966.
- [136] L. Zhu and N. W. Liu, "Multimode resonator technique in antennas: A review," *Electromagnetic Science*, vol. 1, no. 1, article no. 0010041, 2023.



Wen-Jun Lu was born in Jiangmen, Guangdong Province, China, in 1978. He received the Ph.D. degree in electronics engineering from the Nanjing University of Posts and Telecommunications (NUPT), Nanjing, China, in 2007. Since 2013, he has been a Professor with the Jiangsu Key Laboratory of Wireless Communications, NUPT, where he is serving as a Vice Director. His research interests include antenna theory, antenna design, antenna arrays, and wireless channel modeling.

He has advanced generalized odd-even mode theory (GO-EMT) and developed mode synthesis antenna design approach. He has invented the design approach for planar endfire circularly polarized antennas (PECPAs). He is the translator of the Chinese version of *The Art and Science of Ultrawideband Antennas* (the 1st edition, by H. Schantz). He has authored three books, *Antennas: Concise Theory, Design and Applications* (in Chinese, 2014), its 2nd edition *Concise Antennas* (in Chinese, 2020),

and *Multi-mode Resonant Antennas: Theory, Design and Applications* (CRC Press, 2022). He has authored or co-authored over 200 technical papers published in peer-reviewed international journals and conference proceedings. He is the inventor and co-inventor of over 50 granted Chinese patents and 3 granted USA patents. He was a recipient of the Exceptional Reviewers Award of the *IEEE Transactions on Antennas and Propagation* in 2016 and from 2020 to 2023 and the Outstanding Reviewers Award of the *AEÜ: Int. J. of Electronics and Communications* in 2018. He was a co-recipient of the Technological Innovation Award (2-ranked) of the Ministry of Education of China in 2019 for contributions to body-area wireless channel modeling. He has been serving as an Editorial Board Member of the *International Journal of RF and Microwave Computer-aided Engineering* since 2014, an Associate Editor of the *Electronics Letters* since 2019, and an Editorial Board Member of the *Journal of Microwaves* since 2023. He is a Senior Member of the IEEE and the Chinese Institute of Electronics (CIE). He is a Committee Member of the Antenna Chapter and the EMC Chapter of the CIE. He was awarded the title of "the New Century Excellent Talents in Universities" by the Ministry of Education of China in 2012. His Ph.D. dissertation was nominated as one of the Top-100 outstanding Ph.D. dissertations of China in 2009. (Email: wjlu@njupt.edu.cn)